

Estimates of Shear-Wave Q and κ_0 for Unconsolidated and Semiconsolidated Sediments in Eastern North America

by Kenneth W. Campbell

Abstract Measured and calculated values of the effective quality factor Q_{ef} and the site attenuation parameter κ_0 for unconsolidated and semiconsolidated sediments in eastern North America (ENA) indicate that the latter is strongly dependent on sediment thickness. Estimates of κ_0 for National Earthquake Hazard Reduction Program (NEHRP) BC site profiles (sediment plus hard rock) in the Mississippi Embayment and the Atlantic Coastal Plain were found to increase from about 9 to 31 msec for sediment thicknesses ranging from 116 to 600 m. Stochastic simulations using the 175 m thick hypothetical NEHRP BC site profile used to estimate ENA ground motions in the national seismic hazard maps by the U.S. Geological Survey (USGS) indicate that $\kappa_0 = 20$ msec provides a smaller estimate of amplification that agrees more closely with the low-strain short-period site coefficients in the NEHRP Recommended Provisions for Seismic Regulations for New Buildings and Other Structures (NEHRP Provisions) than the 10 msec value used by the USGS. A linear regression of the κ_0 estimates compiled in this study indicates that $\kappa_0 = 20$ msec corresponds to a relatively thick BC sediment thickness of 460 ± 116 m. These same stochastic simulations indicate that the relatively shallow USGS site profile provides estimates of amplification that are smaller than the low-strain long-period site coefficients in the NEHRP Provisions. The dependence of both site attenuation and site amplification on sediment thickness suggests that the use of a single reference site condition for hazard mapping might not be appropriate. Instead, these results imply that either a regional set of reference site profiles should be developed or that a more uniform site condition such as hard rock should be used to define a more stable reference site condition in ENA.

Introduction

The U.S. Geological Survey (USGS) defines the reference site condition used in the development of the national seismic hazard maps as the boundary between the National Earthquake Hazard Reduction Program (NEHRP) site classes B and C (Frankel *et al.*, 1996, 2002; Petersen *et al.*, 2008). The USGS refers to this site condition as either firm rock or the NEHRP BC boundary. It corresponds to a site with a time-averaged shear-wave (S -wave) velocity V_{S30} of 760 m/sec in the top 30 m of the site. The Building Seismic Safety Council (BSSC) uses the USGS hazard maps as the basis for developing seismic design maps in the NEHRP Recommended Provisions for Seismic Regulations for New Buildings and Other Structures (Building Seismic Safety Council [BSSC], 2004), which are subsequently adopted for use in engineering practice by the American Society of Civil Engineers (ASCE, 2006) and in the International Building Code of the International Code Committee (ICC, 2006). Ground motions on other site conditions are estimated by multiplying the mapped BC ground motions that are conservatively assumed to represent NEHRP B site conditions in

these codes, by site coefficients that represent the following five site classes defined primarily in terms of S -wave velocity: A, $V_{S30} > 1500$ m/sec; B, $V_{S30} = 760\text{--}1500$ m/sec; C, $V_{S30} = 360\text{--}760$ m/sec; D, $V_{S30} = 180\text{--}360$ m/sec; and E, $V_{S30} < 180$ m/sec. As a result, it is crucial that the mapped ground motions in eastern North America (ENA) represent a BC site profile that has site-response characteristics that are consistent with those used to develop the NEHRP site coefficients, notwithstanding the fact that they are based on ground-motion data and site conditions typical of western North America (WNA) or more specifically, of California (Borcherdt, 1994; Dobry *et al.*, 2000).

Most of the contemporary ground-motion prediction equations (also known as attenuation relationships or ground-motion models) that are used to estimate peak ground-motion parameters and response spectra in ENA have been developed for hard-rock site conditions (Atkinson and Boore, 1995, 1997; Toro *et al.*, 1997; Somerville *et al.*, 2001; Toro, 2002; Campbell, 2003; Silva *et al.*, 2003; Campbell, 2004; Electrical Power Research Institute [EPRI],

2004; Tavakoli and Pezeshk, 2005). These estimates are then often adjusted to BC site conditions using site amplification factors developed by the USGS for use in the national seismic hazard maps (Frankel *et al.*, 1996, 2002; Petersen *et al.*, 2008). Only a few ground-motion prediction equations have been developed directly for BC site conditions (Atkinson and Boore, 2006; Campbell, 2007; unpublished manuscript, 2009). In either case, stochastic simulations were used to calculate the period-dependent BC amplification factors using the quarter-wavelength method of Joyner *et al.* (1981) and Boore (2003) and the hypothetical S -wave velocity and density BC site profile proposed by Frankel *et al.* (1996). The only difference is that the USGS used a site attenuation parameter κ_0 of 10 msec to adjust the hard-rock ground motions to BC site conditions; whereas, Atkinson and Boore (2006) and Campbell (2007; unpublished manuscript, 2009) used 20 msec in the development of their BC ground-motion prediction equations. Figure 1 demonstrates the impact that different values of κ_0 can have on Fourier spectral site amplifications predicted using the quarter-wavelength method.

In this article, I develop relationships between the effective S -wave quality factor Q_{ef} and S -wave velocity of unconsolidated and semiconsolidated sediments in ENA and use these relationships to estimate κ_0 as a function of sediment depth for representative soil and NEHRP BC sites in the Mississippi Embayment and the Atlantic Coastal Plain. I also show that the low-strain short-period site coefficients in the NEHRP Provisions are consistent with a κ_0 of 20 msec when the USGS hypothetical BC site profile is used to estimate site amplification factors between hard rock and BC site conditions. In order to avoid confusion in what is meant by the terms used to describe the various parts of the site profile in this article, it is useful to define these terms in advance. The term geological profile is used to refer to the total geological structure from the ground surface to a depth

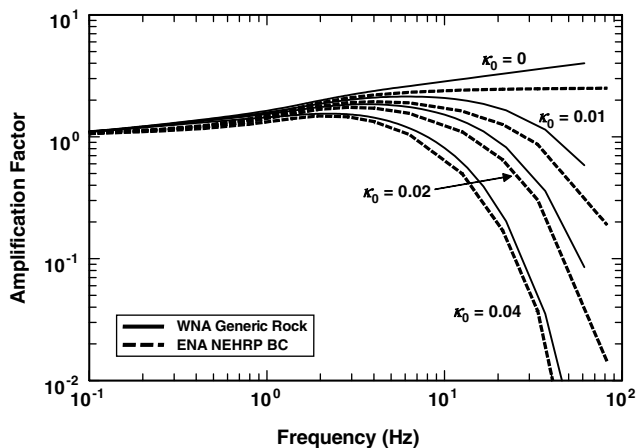


Figure 1. Site amplification of Fourier amplitude spectra for the WNA generic-rock profile of Boore and Joyner (1997) and the hypothetical ENA BC site-profile of Frankel *et al.* (1996). Site factors were calculated using the quarter-wavelength method (Joyner *et al.*, 1981; Boore, 2003). The different curves show the effect of the site attenuation parameter κ_0 (in sec).

corresponding to the earthquake source region (typically 5–10 km). This is often referred to as the crustal profile in stochastic simulation models (Boore, 2003). The term sedimentary column is used to refer to those deposits that overlie the hard-rock section of the geological profile, where the term hard rock is defined as any material having an S -wave velocity exceeding 2000 m/sec (Atkinson and Boore, 2006). The phrase, BC section of the sedimentary column, is used to refer to that part of the sedimentary column that corresponds to $V_{S30} \geq 760$ m/sec. The combined BC and hard-rock sections of the geological profile are referred to as the BC site profile. Figure 2 gives a graphical description of these terms using a typical S -wave velocity profile for the city of Memphis, Tennessee.

Background

Seismologists have long recognized that the amplitude decay of seismic waves within the Earth's crust, defined herein as the effective attenuation of shear (S) waves (Lay and Wallace, 1995; Sato *et al.*, 2002), can be approximated by an equation of the form (e.g., Futterman, 1962; Knopoff, 1964)

$$A(r, f) = A_0 \exp(-\pi f r / Q_{ef} V_S), \quad (1)$$

where r is distance, f is frequency, Q_{ef} is the effective seismic quality factor of S waves (inverse of seismic attenuation), and V_S is the S -wave velocity of the medium. Seismic attenuation can be thought of as either the fractional loss of energy per cycle of oscillation (e.g., Lay and Wallace, 1995) or the exponential decrease in amplitude with time or

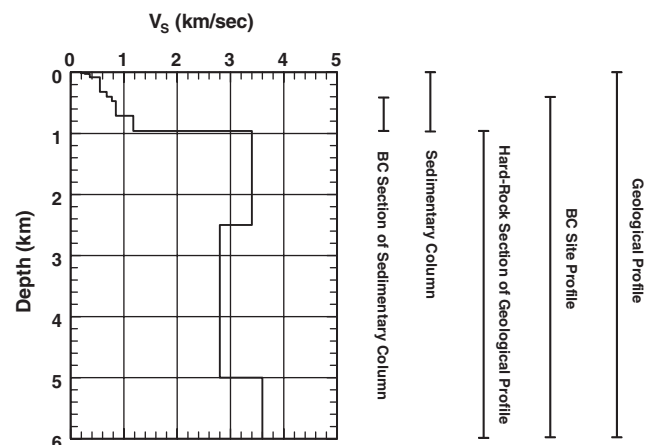


Figure 2. S -wave velocity profile for Memphis, Tennessee, showing the definitions of the site-profile terms used in this study. The velocities for the sedimentary column were taken from Gombert *et al.* (2003) and Cramer *et al.* (2004) and are listed in Table 1. The velocities for the hard-rock section of the geological profile were taken from Andrews *et al.* (1985).

distance (Frankel and Wennerberg, 1987). It is usually divided into two components: a frequency-independent component commonly referred to as intrinsic attenuation or anelasticity (Q_{in}^{-1}), resulting from friction or internal damping, and a frequency-dependent component commonly referred to as scattering attenuation (Q_{sc}^{-1}), resulting from heterogeneities (scatterers) along the travel path (Aki, 1980). Dainty (1981) showed that the effective attenuation can be thought of as the sum of these two attenuation components, given by the equation

$$Q_{ef}^{-1} = Q_{in}^{-1} + Q_{sc}^{-1}. \quad (2)$$

Therefore, if Q_{sc} is frequency-dependent and significantly contributes to the effective attenuation, then Q_{ef} also will be frequency-dependent. Although this attenuation paradigm was developed from surface recordings and applied to attenuation in the lithosphere, Abercrombie (1998) and Kinoshita (2008) have shown that it also applies to borehole recordings. As I will show later, this paradigm leads to estimates of Q_{sc} that are generally equal to or greater than Q_{in} in the thick saturated unconsolidated and semiconsolidated sediments of the Mississippi Embayment and Atlantic Coastal Plain.

Recently, Morozov (2008, 2009) has questioned the $Q_{sc}(f) - Q_{ef}(f)$ paradigm. He suggests that the distinction between a frequency-independent Q_{in} and a frequency-dependent $Q_{sc}(f)$ is confusing and misleading, especially in the context of equation (1). He proposes a geometrical attenuation model that is an alternative to the conventional frequency-dependent attenuation law $Q(f) = Q_0(f/f_0)^\eta$. The new model provides a straightforward differentiation between geometrical and effective attenuation, with the traditional scattering attenuation interpreted in terms of a generally frequency-independent component of geometrical attenuation and an effective attenuation, which he calls Q_e (not to be confused with the effective attenuation Q_{ef} defined in this study) that incorporates the frequency-independent component of intrinsic attenuation and small-scale scattering. Unlike the (Q_0, η) description, the inversion procedure uses only the spectral amplitude data and does not rely on elaborate theoretical models or restrictive assumptions. Data from over 40 reported studies were transformed to this new parameterization. The levels of geometrical attenuation were found to strongly correlate with crustal tectonic types and decrease with tectonic age. The corrected values of Q_e were found to be frequency-independent and generally significantly higher than Q_0 and showed no significant correlation with tectonic age. Several case studies were revisited in detail, including one involving the deep borehole data of Kinoshita (2008) with significant changes in the interpretations. Because Morozov's (2008, 2009) conclusions have not yet been fully vetted by the seismological community, I continue to make the conventional distinction between these two attenuation mechanisms in this article. However, like Morozov (2008, 2009), I interpret the combined intrinsic

and scattering attenuation data in terms of a single frequency-independent quality factor Q_{ef} .

It was not until the early 1980s with the refinement of the stochastic ground-motion simulation method (see Boore [1983] and references therein) that it was recognized that whole-path attenuation within the crust could not completely explain the decay of high-frequency acceleration spectra beyond the source corner frequency, where the acceleration spectrum should be flat according to the commonly accepted ω -square source displacement spectrum (Brune, 1970, 1971). Hanks (1982) suggested that this observed cutoff frequency that he called f_{max} was likely due to site attenuation. Papageorgiou and Aki (1983) suggested that it was primarily a source effect. Without judging which interpretation was correct, Boore (1983) included the effect of this cutoff frequency in his generalization of the stochastic ground-motion simulation method proposed by Hanks and McGuire (1981) by including a high-cut filter in his model of the Fourier acceleration spectrum given by the equation

$$D(f) = [1 + (f/f_{max})^8]^{-1/2}. \quad (3)$$

Around the same time that Hanks (1982) and Papageorgiou and Aki (1983) were debating whether f_{max} was a site attenuation parameter or a source parameter, Cormier (1982) proposed a model in which seismic attenuation could be defined by the rate of the high-frequency decay of the displacement spectrum for frequencies above the corner frequency as the multiplication of two terms: the decay due to the source spectrum f^{-n} and an exponential decay factor $\exp(-\pi t^* f)$. In this model, t^* represents the path-integrated effect of the inverse of the quality factor as defined by the integral (Kanamori, 1967)

$$t^* = \int_{\text{path}} Q_{ef}(r)^{-1} V_S(r)^{-1} dr. \quad (4)$$

Cormier also noted that experimental measures of t^* typically lump scattering effects together with intrinsic anelasticity and combined frequency-dependent attenuation mechanisms together with frequency-independent attenuation mechanisms. Therefore, t^* provides a measure of Q_{ef} rather than Q_{in} or Q_{sc} .

After studying the high-frequency decay of accelerograms recorded in California, Anderson and Hough (1984) suggested that the shape of the acceleration spectrum at high frequencies could be described by an equation similar to Cormier's (1982) that they define as

$$A(f) = A_0 \exp(-\pi \kappa f), \quad f > f_E, \quad (5)$$

where the amplitude A_0 depends on factors such as source properties and propagation distance, κ is a spectral decay parameter, and f_E is a frequency beyond which the fall-off of the spectrum is approximately linear on a plot of the logarithm of $A(f)$ versus f (Fig. 3). According to this

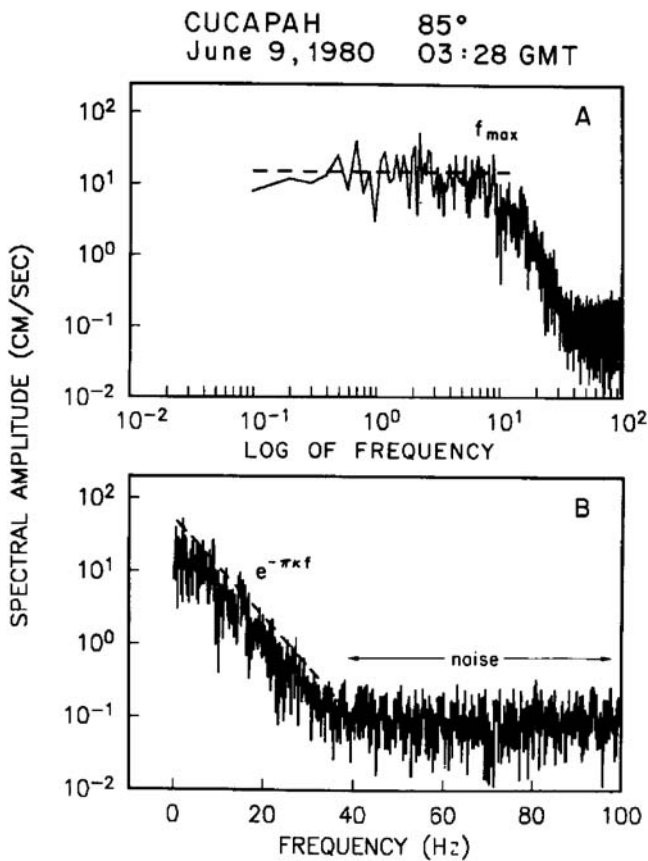


Figure 3. Fourier amplitude spectrum of the N85° E component of ground acceleration recorded at Cucapah during the Mexicali Valley earthquake of 9 June 1980 (M_L 6.2). The accelerograph was a digital recorder that samples at a rate of 200/sec. (A) log-log axes; (B) linear-log axes (after Anderson and Hough, 1984).

equation, the slope of the spectral decay $d \ln A(f)/df$ is $-\pi\kappa$. Anderson and Hough (1984) noted that if $Q_{ef}(r)$ and thus t^* is independent of frequency, the effect of attenuation on a Brune (1970, 1971) source displacement spectrum, for which the high-frequency decay is proportional to f^{-2} , will yield the spectral shape given by both Cormier (1982) and equation (5). These authors further found that κ was dependent on distance with a nonzero intercept that they interpreted to be the attenuation due to the propagation of S waves through the subsurface geological structure and a slope that they interpreted to be the incremental attenuation due to the horizontal propagation of S waves through the crust. They also showed that the spectral decay of the logarithm of the Fourier acceleration spectrum with frequency, assuming an ω -square source spectrum, is flat (i.e., $\kappa = 0$) when $Q_{ef} = \infty$ and $Q_{ef} \propto f$ and is negative (i.e., $\kappa > 0$) when $Q_{ef} = Q_0$ and $Q_{ef} \propto f^\eta$ ($\eta < 1$). However, only when $Q_{ef} = Q_0$ (a constant) is the spectral decay described exactly by equation (5). Fitting equation (5) to a model with a fractional frequency dependence of Q_{ef} will yield a smaller value of κ than a model in which Q_{ef} is assumed to be constant, which emphasizes the importance of the standard assumption

that Q_{ef} is independent of frequency when interpreting κ as a site parameter. Otherwise, the true value of Q_{ef} will be underestimated.

Hough *et al.* (1988) and Hough and Anderson (1988) performed a thorough study of κ using the recordings of small earthquakes from the Anza seismic array in southern California. Based on this analysis, Hough and Anderson (1988) proposed a general model for κ given by the equation

$$\kappa(r) = \int_{\text{path}} Q_i(z)^{-1} V_S(z)^{-1} dr, \quad (6)$$

where Q_i is the frequency-independent component of Q_{ef} at depth z within the profile. They used this model to infer the attenuation structure at Anza from a regional crustal velocity model. They noted that their proposed model for $\kappa(r)$ was the same as that given by Cormier (1982) for t^* in equation (4), except that it used only the frequency-independent component of Q_{ef} . Hough *et al.* (1988) concluded that the similarity of the distance-dependence of $\kappa(r)$ in the Anza and Imperial Valley regions of southern California, areas in which the intercepts at $r = 0$ were very different presumably due to the vastly different subsurface geology, supported the earlier assumption by Anderson and Hough (1984) that the intercept of $\kappa(r)$ represents the attenuation of seismic waves within the geological structure beneath the site and that the distance-dependence of $\kappa(r)$ represents the attenuation due to the horizontal propagation of seismic waves within the crust. Hough *et al.* (1988) referred to this site component of $\kappa(r)$ as κ_0 . Anderson (1991) generalized the linear $\kappa(r)$ model of Hough and Anderson (1988) and Hough *et al.* (1988) by proposing a mathematical formulation of the observed behavior of κ that regarded this parameter to be an arbitrary function of distance that he defined by the equation

$$\kappa(r) = \kappa_0 + \tilde{\kappa}(r), \quad (7)$$

where κ_0 is the intercept at $r = 0$.

Since being introduced, κ_0 has become the preferred parameter for incorporating site attenuation in the calculation of amplification factors using the quarter-wavelength method of Joyner *et al.* (1981). A summary of κ_0 estimates for a variety of geological conditions throughout the United States has been compiled by Anderson (1986, 1991) and Silva and Darragh (1995). Even Halldorsson and Papageorgiou (2005) have adopted it as their high-frequency filter parameter in the revision of the specific barrier model of the earthquake source (Papageorgiou and Aki, 1983) because of its better fit to strong-motion data. However, these latter authors continue to suggest that it could be a source parameter rather than a site parameter.

In the quarter-wavelength method, the site amplification of the Fourier amplitude spectrum of acceleration is calculated from the equation (Boore, 2003)

$$\text{Amp}(f) = (\rho_S \beta_S / \bar{\rho} \bar{\beta})^{1/2} \exp(-\pi \kappa_0 f), \quad (8)$$

where ρ_S and β_S are the density and S -wave velocity at the base of the geological profile, and $\bar{\rho}$ and $\bar{\beta}$ are the time-averaged density and S -wave velocity over a depth equivalent to the quarter-wavelength of a seismic wave of frequency f propagating vertically through the profile. All of the ENA ground-motion estimates used in the 2008 update of the national seismic hazard maps (Petersen *et al.*, 2008) have either been directly or indirectly adjusted to BC site conditions using this equation. Therefore, the discussion of Q_{ef} and κ_0 presented in the remainder of this article is restricted to their use in the quarter-wavelength method. As I will show later, conclusions regarding these attenuation parameters could be quite different in the context of other more complex site amplification methods.

The site amplification factors used by the USGS to estimate BC ground motions from those on hard rock were developed from the quarter-wavelength method using a hypothetical BC site profile with $\kappa_0 = 10$ msec (Frankel *et al.*, 1996). These authors reportedly based this value on a study of borehole recordings by Fletcher (1995). However, Fletcher does not provide specific information regarding the lithology or S -wave velocities of these sediments. As a result, the value of κ_0 (more accurately t^*) determined by Fletcher for this site could not be confirmed as representative of a BC site profile (see the USGS Hypothetical BC Site-Profile section). Atkinson and Boore (2006) used the same velocity and density profile proposed by Frankel *et al.* (1996), except with a κ_0 of 20 msec, to develop their new finite-source stochastic ground-motion prediction equation for ENA; however, they did not explain why they used that particular value in lieu of the original value proposed by Frankel *et al.* (1996). Following Atkinson and Boore (2006), Campbell (2007) also adopted this larger value for κ_0 in a preliminary update of his hybrid-empirical ground-motion prediction equation for ENA. A. Frankel (personal comm., 2007) suggested that, in his opinion, the limited data on κ_0 for BC sites in ENA could not rule out either value as being correct. In the discussion that follows, I will show that κ_0 is strongly dependent on the thickness of the sediments beneath the site and will provide evidence to suggest that the 20 msec value is more appropriate for estimating low-strain short-period ground motions in ENA using the hypothetical USGS BC site profile. I also postulate that the value of κ_0 for the geological structure that underlies a site can be separated into two principal components: one due to the sedimentary column and one due to the hard-rock section of the geological profile that underlies these sediments.

Site Attenuation of Hard-Rock Sites

Hard-Rock Sites in ENA

Silva and Darragh (1995) used a spectral-fitting technique together with the point-source stochastic simulation method to derive empirical estimates of κ_0 for 16 strong-motion recordings on sites described as granitic plutons, car-

bonates, and Precambrian rock of the Canadian Shield. They found a median κ_0 of 7 msec for these sites with individual estimates that ranged between 4 and 16 msec. An earlier version of this study was used by Electrical Power Research Institute (EPRI, 1993) and Toro *et al.* (1997) to select a median κ_0 of 6 msec to use in the development of an ENA hard-rock ground-motion prediction equation using the point-source stochastic simulation method. Atkinson (1996) proposed an upperbound value of 4 msec for the Canadian Shield based on the spectral decay of Fourier acceleration spectra over frequencies of 4–30 Hz from small earthquakes recorded on the Eastern Canadian Telemetered Network (ECTN). Based in part on the study by Atkinson (1996), Beresnev and Atkinson (1999) used a median κ_0 of 2 msec in their estimation of hard-rock ground motions using a finite-source stochastic simulation model. However, these authors also used a site amplification factor of unity and a subevent stress drop of 50 bars, consistently smaller than contemporary estimates of these parameters in ENA (e.g., Atkinson and Boore, 2006), which likely compensated for the use of a relatively small κ_0 value.

Close inspection of Atkinson's (1996) figure 7 suggests that κ_0 could be as high as 7 msec over the 12–22 Hz frequency range for which the observed spectral decay appears to be less impacted by possible high-frequency noise and low-frequency source and site effects. It is also possible that the ECTN sites in the Canadian Shield, which are sited directly on hard, glacially scoured Precambrian rock (Beresnev and Atkinson, 1997), are underlain by higher quality rock than the average hard-rock site used by Silva and Darragh (1995). Anderson and Hough (1984), Anderson (1986, 1991), and Anderson *et al.* (1996) show that rock quality can have a significant impact on the value of κ_0 . Barton (2007) gives similar evidence for the quality factor. A specific example for ENA is given by Atkinson (1996) who found relatively large κ_0 values of 20–40 msec for ECTN sites in the Charlevoix and Sudbury areas of southeastern Canada that are reported to be located on fractured Precambrian rock within an ancient meteor impact crater. Similarly, Silva and Darragh (1995) found a κ_0 of 25 msec from strong-motion recordings of the 1988 Nahanni earthquake sequence on sheared rock. These later results are also consistent with the results of laboratory experiments on hard rock that have shown that the more fractured a rock is, the lower the quality factor (e.g., Johnston *et al.*, 1979; Johnston and Toksoz, 1980b; Barton, 2007).

Chapman *et al.* (2003) analyzed the spectral decay of 25 recordings located approximately 10 km from a swarm of very shallow (0.1–2.4 km deep) microearthquakes at Monticello Reservoir, South Carolina, in an attempt to estimate κ . The earthquakes and the recording site were located within a complex metamorphic terrane intruded by plutons of granite and granodiorite composition. They used a spectral-fitting technique similar to that of Silva and Darragh (1995) to determine a median κ that ranged from –4 to 18 msec for upper frequency limits from 15 to 40 Hz (the high-frequency limit

of the data). They attributed the higher values of κ to a bias caused by the relatively low (15–25 Hz) spectral corner frequencies of the recordings and concluded that the true value of κ was too small to be resolvable from the data (i.e., $\kappa \leq 10$ msec). [Silva and Darragh \(1995\)](#) interpreted several microearthquake recordings at Monticello Reservoir at epicentral distances of 1–8 km and found a κ_0 of 13–16 msec.

[Atkinson and Boore \(2006\)](#) made a careful examination of the Fourier acceleration spectra compiled by [Atkinson \(2004\)](#) and found that these data were consistent with individual estimates of κ_0 that ranged from 0 (no attenuation) to 10 msec with a median value of 5 msec. The database consisted of 1700 digital seismograms from 186 earthquakes (m_N 2.5–5.6) that occurred in southeastern Canada and northeastern United States from 1990 to 2003. These data were recorded on short-period ECTN seismographs and on broadband seismographs of the Canadian National Seismographic Network and the U.S. National Seismic Network on hard-rock sites that were reported to have near-surface S -wave velocities in excess of 2000 m/sec. (e.g., [Beresnev and Atkinson, 1997](#)).

Hard-Rock Sites at Anza

In order to show that the small values of κ_0 reported for ENA hard rock in the preceding section are not unrealistic, it is useful to compare them with estimates from a region near Anza that some seismologists consider might be a WNA analogy to the hard-rock environment of ENA (e.g., [Silva et al., 1999b](#)). The Anza seismic array is located within the southern California batholith, a region of massive granitic rock within the peninsular ranges of southern California. Two of these sites, the Piñon Flat Observatory (PFO) and Keenwild (KNW), are located on granitic plutons away from any active traces of the San Jacinto fault zone. Deep boreholes drilled near PFO and KNW have respective S -wave velocities in excess of 1600 and 1900 m/sec (nearly equal to hard rock) at depths below 15 and 20 m and S -wave velocities of 2600 and 3000 m/sec at depths below 50 m ([Fletcher et al., 1990](#)). The more highly weathered rock above depths of 15 and 20 m for PFO-BH (borehole sites from the nearby array sites) and KNW-BH has a much lower velocity of approximately 800 m/sec. The array instrument at PFO is located on a pier in a buried vault, and the KNW array instrument is located on a concrete pad on an outcrop of competent rock. Therefore, the array stations can be considered to be less impacted by the weathered zone and can be used to estimate the response of hard rock for purposes of this study.

Using the spectral decay method, [Anderson \(1991\)](#) calculated a κ_0 of 2 msec for KNW and 4 msec for PFO based on the distance-dependence of $\kappa(r)$ that he interpreted in terms of equation (7). [Silva and Darragh \(1995\)](#) calculated a κ_0 of 6 msec for these two sites directly from the recorded spectra using a spectral-fitting technique. Based on data given in [Anderson \(1991\)](#), I calculated an average κ_0 of 7 msec for the six sites of the Anza array where hard rock was encoun-

tered at relatively shallow depths. These values are similar to κ_0 values found for hard-rock sites in ENA. [Fletcher et al. \(1990\)](#) used vertical seismic profiling (VSP) to estimate a t^* of 4 msec ($\bar{Q}_{ef} = 8$) for KNW-BH and 3 msec ($\bar{Q}_{ef} = 11$) for PFO-BH over the top 50 m, although they note that their results could be contaminated by near-surface attenuation and interference effects. [Aster and Shearer \(1991\)](#) inverted uphole–downhole spectral ratios in the 2–100 Hz frequency band using generalized reflection–transmission modeling to estimate $\bar{Q}_{ef} = 9$ over depths of 0–150 m and 27 over depths of 150–300 m from 20 small earthquakes recorded at KNW-BH. Their comparison of spectral ratios between the surface instrument at KNW and the 300 m deep instrument at KNW-BH yielded $t^* = 11$ m sec in the top 300 m at KNW. This value is more than double what others have estimated at KNW using the spectral decay method.

[Aster and Shearer \(1991\)](#) noted that the P -wave quality factor was less than or equal to the S -wave quality factor in the upper 300 m at KNW-BH, which they interpreted to be an indication that near-surface scattering attenuation is at least as significant as intrinsic attenuation (e.g., [Anderson et al., 1965](#); [Kang and McMechan, 1994](#)). [Vernon et al. \(1998\)](#) came to the same conclusion from analysis of data recorded by a dense seismic array deployed in the vicinity of PFO-BH that they attributed to strong scattering of incident body-wave signals into a complex mishmash of body-wave and surface-wave modes within the near-surface zone of weathered rock. [Dainty \(1981\)](#) assumed that Q_{in} was independent of frequency and that Q_{sc} was proportional to frequency for frequencies above 1 Hz, and others have followed his example (e.g., [Pulli, 1984](#); [Fehler et al., 1988](#); [Kang and McMechan, 1994](#)). These assumptions are typically made in efforts to interpret coda- Q measurements for which the variation of coda- Q with frequency is thought to reflect scattering effects (e.g., [Aki and Chouet, 1975](#); [Morozov, 2008](#)). If Q_{sc} is indeed proportional to frequency, it will not contribute to the value of κ_0 calculated from the spectral decay method ([Anderson and Hough, 1984](#)), and the resulting κ_0 will represent only intrinsic attenuation. This could explain the discrepancy between the larger value of t^* found by [Aster and Shearer \(1991\)](#) at KNW compared to the κ_0 values found by [Anderson \(1991\)](#) and [Silva and Darragh \(1995\)](#), both of which used the spectral decay method proposed by [Anderson and Hough \(1984\)](#). If this is the case, these latter estimates might be a measure of intrinsic rather than effective attenuation. The same is true for other estimates of site attenuation using the spectral decay method. However, if [Morozov \(2008, 2009\)](#) is correct, then the value of κ_0 derived from the spectral decay method will give a true estimate of effective attenuation.

Hard-Rock κ_0 in ENA

Based on the results presented in the preceding sections, I selected 5 msec as the value of κ_0 to use for the hard-rock component of site attenuation. This value is consistent with

the median value found by Atkinson and Boore (2006) for southeastern Canada and the northeastern United States and falls in the middle of the range of hard-rock values presented in the previous sections. In order to justify adding this hard-rock κ_0 to that of the overlying sediments, I assume that it corresponds to a geological or BC site profile that is much thicker than the overlying sediments. Hough and Anderson (1988) estimated this thickness to be at least 5 km, based on the results of their inferred Q_i structure at Anza. However, there are two issues that remain before this 5 msec value can be used as an estimate of hard-rock κ_0 at depth: (1) the potential contamination of near-surface scattering effects and (2) the potential impact of the overburden.

Laboratory and field measurements suggest that the attenuation in near-surface rocks where hydrostatic pressures are relatively low is not simply dependent on rock type but is dominated by an increase in fracture content and other heterogeneities that can lead to wave scattering (Abercrombie, 1997, 1998). However, the sites used by Atkinson and Boore (2006) to estimate κ_0 are underlain by hard, glacially scoured rock of the Canadian Shield with near-surface S -wave velocities generally exceeding 2000 m/sec. These sites are not likely to be contaminated by significant fracturing and scattering effects that might otherwise be attributable to near-surface weathered or highly-fractured rock. Furthermore, if Q_{sc} is proportional to frequency, as some seismologists have proposed, estimates of κ_0 at hard-rock sites in ENA, all of which have been calculated using the spectral decay method, will not include scattering effects (Anderson and Hough, 1984). This might have been the cause of the conflicting results at Anza where use of the spectral decay method yielded κ_0 values that ranged between 3 and 6 msec for the entire geological profiles underlying PFO and KNW; whereas, the spectral-ratio method, which includes intrinsic and scattering attenuation, yielded a value of 11 msec for the upper 300 m at KNW alone. Some seismologists have developed theories or alternative means of data analysis that predict both intrinsic and scattering attenuation are independent of frequency, at least up to frequencies of engineering interest (Frankel and Clayton, 1986; Wennerberg and Frankel, 1989; Morozov, 2008, 2009). Frankel and Wennerberg (1987) proposed an energy-flux model that predicts the quality factor determined from the decay rate of the coda is more sensitive to intrinsic attenuation than to scattering attenuation, which contradicts the basic assumption of most scattering models. If this is true, the only consequences to the present study are that the hard-rock estimates of κ_0 based on the spectral decay method might incorporate near-surface scattering effects as well as intrinsic anelasticity, which could cause an overestimate of the effective attenuation at depth. However, earthquake and laboratory studies indicate that this is not likely to be the case.

Earthquake and laboratory studies have shown that the relatively shallow depths of overburden typically found in ENA do not have a large influence on attenuation. Laboratory experiments conducted by Johnston *et al.* (1979) and

Johnston and Toksoz (1980a) found that the quality factor and the seismic velocity of hard sandstone and limestone with $V_S > 2000$ m/sec increased with confining pressure up to about 500–1000 bars, after which they became relatively independent of pressure. Assuming depths of overburden less than 1000 m in ENA, the hydrostatic pressure at the bottom of the sedimentary column is no greater than about 150 bars. This represents confining pressures where Johnston and Toksoz (1980a) found the smallest quality factors. The increase of the quality factor with hydrostatic pressure has also been found to be larger for dry rocks than for saturated rocks (e.g., Gardner *et al.*, 1964; Johnston and Toksoz, 1980a), which has implications for the attenuation in saturated sediments such as those found in the Mississippi Embayment and the Atlantic Coastal Plain. The increase in the quality factor with confining pressure has been interpreted as resulting from the closure of fractures. Johnston *et al.* (1979) and Johnston and Toksoz (1980a, 1980b) also found that at relatively low confining pressures, friction at fractures is the most probable dominant mechanism of intrinsic attenuation in laboratory specimens. Fractures are also major scatterers of seismic energy at wavelengths smaller than the dimensions of the fractures, which suggests that high-frequency scattering will also decrease with increasing hydrostatic pressure as the fractures are closed (e.g., Johnston and Toksoz, 1980b). This has been shown to be the case for earthquake recordings. For example, Mori and Frankel (1991) observed a significant decrease in scattering attenuation below about 5 km (hydrostatic pressure of ~ 1000 bars) in southern California, the same depth where Hough and Anderson (1988) found the quality factor to reach its maximum value at Anza. Moos and Zoback (1983) also found that the seismic velocity (rock quality) of crystalline rocks in deep boreholes at the Monticello Reservoir and the California Mojave Desert decreased with increasing fracture density.

Proposed Method of Estimating Site Attenuation

There are very few direct measurements of κ_0 at sedimentary sites in ENA. Liu *et al.* (1994) analyzed high-quality, three-component digital seismograms recorded at 27 Mississippi Embayment stations of the Portable Array for Numerical Data Acquisition (PANDA) seismic array located at epicentral distances of 0–100 km from 94 earthquakes with magnitudes of m_{Lg} 1.3–3.6. They determined κ at each station from the spectral decay of the Fourier amplitude spectra for the 5–25 Hz frequency band by fitting the linear equation (Anderson and Hough, 1984)

$$\kappa_{ij}(r) = \kappa_{0i} + \kappa_1 r_{ij}, \quad (9)$$

where $\kappa_{ij}(r)$ and r_{ij} are the observed spectral decay parameter and epicentral distance at station i from event j , κ_0 is the intercept corresponding to the site attenuation parameter for station i , and κ_1 is the slope of the regression equation

corresponding to the dependence of attenuation on distance. They found κ_0 values for the sedimentary column that ranged from 21.3 to 48.3 msec for sites with sediment thicknesses of 463 to 715 m.

[Silva and Darragh \(1995\)](#) analyzed three ENA strong-motion recordings using the spectral-fitting technique at sites described as sandstone and claystone and found a median κ_0 of 17 msec with individual estimates that ranged between 15 and 18 msec. They described these sites as “ENA soft rock” but considered them to represent NEHRP BC site conditions according to the site classes defined in the NEHRP Provisions ([BSSC, 2004](#)). Based on these estimates and a relationship between κ_0 and V_{S30} developed from WNA data, [Silva et al. \(1999b\)](#) concluded that $\kappa_0 = 20$ msec was a realistic value to use for relatively deep BC sites typical of sandstones of the Gulf Coast region and mudstones, claystones, and siltstones of South Carolina and the Colorado Denver Basin. They suggested that the 10 msec value recommended by [Frankel et al. \(1996\)](#) for characterizing BC sites in the national seismic hazard maps is probably too low unless these sites are underlain by very hard-rock ($V_S > 2500$ m/sec) at very shallow depths (≤ 91 m).

[Chapman et al. \(2003\)](#) found a κ_0 of 49 msec for a 775 m thick sedimentary column centered near Summerville, South Carolina, using weak-motion recordings at four stations located in the Middleton Place—Summerville seismic zone from 26 earthquakes with magnitudes ranging from 0.9 to 2.4. The area is located in the Atlantic Coastal Plain approximately 25 km northwest of Charleston. The sediments had an average S -wave velocity of 700 m/sec. Two of the seismometers were located in boreholes at depths of 62 and 83 m. These authors used the average time intervals between the direct S and the surface-reflected S at these two stations to estimate average S -wave velocities of 564 and 535 m/sec for the overlying sediments. Estimates of κ_0 were estimated from the direct S and Sp converted phases using the spectral-fitting technique for frequencies ranging from 1 to 30 Hz and from 10 to 25 Hz with virtually identical results. The travel time of S waves through the sediments was estimated to be 1.10 sec, yielding $\bar{Q}_{ef} = 22.4$ from equation (12). The estimated quality factor for P -waves was less than this value, inferring that scattering attenuation was at least as great as intrinsic attenuation.

All of the remaining estimates of κ_0 for sedimentary and BC sites presented in this article were calculated from the following relationship modified from [Hough and Anderson \(1988\)](#) and [Chapman et al. \(2003\)](#):

$$\kappa_0 = \int_0^z Q_{ef}(z)^{-1} V_S(z)^{-1} dz, \quad (10)$$

where $Q_{ef}(z)$ and $V_S(z)$ are the effective quality factor and S -wave velocity at a depth z within the profile. This relationship is consistent with equation (6), except that it isolates the contribution due to the sediments. By stripping off those sediments in the upper part of the sedimentary column that have

$V_{S30} < 760$ m/sec, this relationship also can be used to estimate the value of κ_0 for the BC section of the sedimentary column. Equation (10) implicitly assumes that the value of $Q_{ef}(z)$ within the sedimentary column is independent of frequency, which is also a basic assumption of all site-response methodologies (e.g., [Kramer, 1996](#)). There is evidence to support the assumption of frequency-independent attenuation in sediments. [Anderson and Hough \(1984\)](#), [Hough et al. \(1988\)](#), and [Morozov \(2008\)](#) give seismological evidence to suggest that $Q_{ef}(z)$ at high frequencies is approximately independent of frequency in the shallow crust. [Wennerberg and Frankel \(1989\)](#) showed theoretically that a frequency-dependent mechanism of attenuation within a sedimentary sequence that extends from the surface to a depth of several kilometers can result in a quality factor that is approximately constant with frequency between 0.2 and 200 Hz. [Wang et al. \(1994\)](#) showed that estimates of the quality factor from critically refracted pulses generated using a plank and hammer were independent of frequency for frequencies of 10–70 Hz. [Gibbs et al. \(1994\)](#) found a similar result from spectral ratios of synthetic VSP and weak-motion data. [Abercrombie \(1997\)](#) found that borehole recordings at depths of 0–2900 m were consistent with a quality factor that was independent of frequency over the 3–100 Hz useable bandwidth of the data. Although it is commonly accepted that attenuation in sediments is generally independent of frequency, [Abercrombie \(1997\)](#) and [Kinoshita \(2008\)](#) have interpreted deep borehole recordings in California and Japan as having a frequency-dependent $Q_{ef}(z)$. However, [Morozov \(2008\)](#) has shown that the Japan data can be reinterpreted as having a frequency-independent $Q_{ef}(z)$. Regardless of whether attenuation in sediments is frequency-dependent or frequency-independent, as discussed previously, any frequency-dependent attenuation effects that might be present are neglected in the application of equation (10).

It is useful to quantify the path-averaged value of $Q_{ef}(z)$ that corresponds to a specified value of κ_0 in order to compare it with values obtained from other studies. For a sedimentary profile of a given thickness, equation (10) can be expressed as ([Boore, 2003](#))

$$\kappa_0 = H / \bar{Q}_{ef} \bar{V}_S, \quad (11)$$

where H is the thickness, \bar{Q}_{ef} is the average effective quality factor, $\bar{V}_S = H/t_r$ is the time-averaged S -wave velocity of the sediments, and t_r is the vertical travel time of the S waves of the sediments. Substituting the expression for \bar{V}_S into equation (11) and solving for \bar{Q}_{ef} , results in the following equation for the average quality factor:

$$\bar{Q}_{ef} = H / \kappa_0 \bar{V}_S = t_r / \kappa_0. \quad (12)$$

The proposed method of estimating κ_0 from equation (10) is demonstrated using a representative sedimentary column for the Memphis area developed from data provided in [Gomberg et al. \(2003\)](#) and [Cramer et al. \(2004\)](#). These

investigators used in situ *S*-wave velocity measurements to estimate the average velocity for the major geologic units that underlie Memphis and the surrounding region of Shelby County. They used these estimates to construct a grid of sedimentary columns that they used, together with 1D equivalent-linear site-response analyses, to incorporate site effects in the development of a regional probabilistic seismic hazard map. Table 1 gives a typical 960 m sedimentary column for downtown Memphis (uplands area) that I derived from data used in these studies. The thickness of each of the geologic units was taken as the average of the range of thicknesses given in Gombert *et al.* (2003). The estimates

of *S*-wave velocity were taken from Cramer *et al.* (2004) and are generally similar to the average values given in Gombert *et al.* (2003). The resulting value of κ_0 calculated from equation (10) using estimates of Q_{ef} reported by Cramer *et al.* (2004) is 48.2 msec ($\bar{Q}_{ef} = 29.1$) for the 960 m sedimentary column. The value for the geological profile is estimated to be 53.2 msec after adding the inferred value of 5 msec for the hard-rock section of the geological profile. The corresponding values of κ_0 for the 564 m BC section of the sedimentary column, and the corresponding BC site profiles are 11.9 msec ($\bar{Q}_{ef} = 49.5$) and 16.9 msec, respectively. The results are summarized in Table 1.

Table 1
Site Attenuation Parameters for a Representative Geological Profile in Downtown Memphis*

Unit/Formation (Age)	Description	Depth (m)	Thickness (m)	V_S (m/sec)	Cramer		Boore and Joyner		Intermediate	
					Q_{ef}	κ_0 (msec)	Q_{ef}	κ_0 (msec)	Q_{ef}	κ_0 (msec)
Loess (Pleistocene)	Eolian, unconsolidated, poorly stratified glacial silts and sands	0	12	191	10	6.28	10	6.28	10	6.28
		-	0			0		0		0
Lafayette formation (Pleistocene and Pliocene)	Indurated clay, silt, sand, gravel and cobbles, locally cemented	12	12	268	25	1.79	10	4.48	15	2.99
		-	0			0		0		0
Upper Claiborne group (Eocene)	Dense clays, silts, and fine sands with organic fragments	24	56	360	25	6.22	10	15.56	20	7.78
		-	0			0		0		0
Memphis sand (Eocene)	Fine to coarse sands, interbedded with silt and clay	80	240	550	25	17.45	10	43.64	20	21.82
		-	0			0		0		0
Flour Island formation (Paleocene)	Dense clays, with fine-grained sands and lignite	320	80	675	25	4.74	10	11.85	20	5.93
		0	4			0.24		0.59		0.30
Fort Pillow sand (Paleocene)	Well-sorted sands with minor silt, clay, and lignite horizons	400	70	775	50	1.81	20	4.52	30	3.01
		4	70			1.81		4.52		3.01
Old Breastworks formation (Paleocene)	Dense clays and silts, with some sands and organic layers	470	240	850	50	5.65	50	5.65	50	5.65
		74	240			5.65		5.65		5.65
Sedimentary rock (Cretaceous)	Undifferentiated sediments	710	250	1175	50	4.26	50	4.26	50	4.26
		314	250			4.26		4.26		4.26
Hard rock (Paleozoic and older)	Limestone and crystalline rock	960	5–10 km	3400	-	5.0	-	5.0	-	5.0
		564								
Sedimentary column	-	-	960	-	29.2	48.2	14.6	96.2	24.3	57.7
		-	564	-	49.4	11.9	39.4	15.0	44.8	13.2
Geological profile	-	-	5–10 km	-	-	53.2	-	101.2	-	62.7
		-		-		16.9		20.0		18.2

*Note: Values in italics represent the BC section of the sedimentary column. The values for Q_{ef} were taken from data provided by Cramer *et al.* (2004) and Boore and Joyner (1991); all other data were taken from Gombert *et al.* (2003) and Cramer *et al.* (2004). Intermediate Q_{ef} values are intermediate to those of Cramer and Boore and Joyner. The values of κ_0 for each layer were calculated from equation (10).

Although the S -wave velocities assigned to each of the geologic units in the Memphis site profile are relatively well constrained by actual measurements, the values of Q_{ef} are not. The only justification that [Cramer *et al.* \(2004\)](#) give for their specific selection of quality factors is that site amplification is not very sensitive to $Q_{ef} \geq 10$ and that the values of Q_{ef} in the region have been determined to be no less than 20 to 40 by [Pujol *et al.* \(2002\)](#). In order to test the sensitivity of the calculated value of κ_0 to the assumed Q_{ef} profile, I repeated the calculation using the Q_{ef} values that [Boore and Joyner \(1991\)](#) assigned to a deep-soil profile in ENA based on ground-motion recordings in the Mississippi Embayment. The resulting κ_0 values are 96.2 msec ($Q_{ef} = 14.6$) for the sedimentary column and 101.2 msec for the geological profile (Table 1). These latter estimates are nearly a factor of 2 higher than those based on the Q_{ef} profile of [Cramer *et al.* \(2004\)](#). However, most of this difference comes from the differences in Q_{ef} assigned to the softer soil deposits. The κ_0 values calculated for the BC section of the sedimentary column and the corresponding BC site profile using the Q_{ef} values given by [Boore and Joyner \(1991\)](#) are 15.0 msec ($Q_{ef} = 39.4$) and 20.0 msec, respectively. These values are only 20%–25% higher than the BC values derived from the Q_{ef} profile used by [Cramer *et al.* \(2004\)](#).

[Wen and Wu \(2001\)](#) report a κ_0 of 63 msec for the sedimentary column beneath Memphis that C. Wu (personal comm., 2008) attributes to the following relationship between Q_{ef} and depth developed by R. Herrmann and A. Akinci (see [Data and Resources](#) section) from ground-motion measurements in the Mississippi Embayment:

$$Q_{ef}(z) = 6z^{0.24}. \quad (13)$$

This value of κ_0 falls between the estimates derived from the two Q_{ef} profiles described in the previous paragraph. In fact, the value of κ_0 reported by [Wen and Wu \(2001\)](#) is closely matched by simply using Q_{ef} values that are intermediate between those of [Boore and Joyner \(1991\)](#) and [Cramer *et al.* \(2004\)](#) for sediments of similar S -wave velocity. Using this intermediate Q_{ef} profile, I obtained a κ_0 of 57.7 msec ($Q_{ef} = 24.3$) for the sedimentary column and 62.7 msec for the geological profile (Table 1). The κ_0 values for the 564 m BC section of the sedimentary column and the corresponding BC site profile are 13.2 msec ($Q_{ef} = 44.8$) and 18.2 msec, respectively. Additional support for using the intermediate Q_{ef} profile comes from earthquake studies that have found a path-averaged Q_{ef} for the entire Mississippi Embayment sedimentary column that ranges between 20 and 36 ([Wuenscher *et al.*, 1991](#); [Chen *et al.*, 1994](#); [Liu *et al.*, 1994](#); [Langston, 2003b](#)). Similar values have also been found for other sedimentary basins located both inside and outside of the United States ([Hauksson *et al.*, 1987](#); [Clouser and Langston, 1991](#); [Chapman *et al.*, 2003](#); [Langston, 2003a,b](#); [Kinoshita, 2008](#)).

The similarity in the three estimates of κ_0 for the Memphis BC site profile is due largely to the agreement

in the value of the quality factor ($Q_{ef} = 50$) for the deeper sediments. Other earthquake and laboratory studies have found that low-strain values of Q_{ef} and Q_{in} range anywhere from 20 to as large as 100 for semiconsolidated sediments similar to those in the deeper parts of the Mississippi Embayment ([Johnston *et al.*, 1979](#); [Johnston and Toksoz, 1980a,b](#); [Chang *et al.*, 1992](#); [Liu *et al.*, 1994](#); [Lay and Wallace, 1995](#); [Chapman *et al.*, 2003](#); [Langston *et al.*, 2005](#); [Assimaki *et al.*, 2008](#)). In order to test the sensitivity of κ_0 to this value, I repeated the calculation for the Memphis profile substituting Q_{ef} values of 25 and 100 in place of 50 for the deeper sediments. These calculations indicate that κ_0 for the BC site profile varies by about -25% to $+55\%$ for this factor of 2 difference in Q_{ef} . There is also uncertainty associated with layer thicknesses and S -wave velocities. However, these parameters are taken from profiles provided by individual investigators, and their uncertainty is assumed to be adequately captured by these investigations.

Estimates of Q_{ef} for Sedimentary Deposits

Models Used to Estimate Q_{ef}

Because of the relatively large sensitivity of κ_0 to the Q_{ef} profile, I chose to include uncertainty in Q_{ef} by proposing four models that are intended to capture its variability at both low S -wave velocities (shallow depths) and high S -wave velocities (large depths). Model 1 is based on Q_{ef} values that are intermediate to the profiles proposed by [Boore and Joyner \(1991\)](#) and [Cramer *et al.* \(2004\)](#). As shown in the previous section, the values from these investigators appear to serve as reasonable end members of an intermediate Q_{ef} profile that results in a κ_0 for the Memphis sedimentary column that agrees with a relationship developed from actual measurements (R. Herrmann and A. Akinci, see [Data and Resources](#) section). An eyeball fit of these Q_{ef} values on S -wave velocity resulted in the equation

$$Q_{ef} = 7.17 + 0.0276 V_S, \quad (14)$$

where V_S is S -wave velocity in m/sec. Model 2 uses this same equation except that it constrains Q_{ef} to 50 when $V_S > 800$ m/sec in order to be consistent with the same constraints imposed by [Boore and Joyner \(1991\)](#) and [Cramer *et al.* \(2004\)](#).

Model 3 is based on the empirical Q_{ef} and V_S versus depth relationships developed by R. Herrmann and A. Akinci (see [Data and Resources](#) section). Their model for V_S is given by the equation

$$V_S = 250z^{0.18}, \quad (15)$$

where z is depth in meters. In order to make this relationship more generally applicable to other site profiles, I combined it with the Q_{ef} relationship in equation (13) developed by these same investigators (R. Herrmann and A. Akinci, see [Data and Resources](#) section) to derive the equation

$$Q_{\text{ef}} = \begin{cases} 10 & V_S \leq 366 \text{ m/sec} \\ 0.00382 V_S^{1.333} & V_S > 366 \text{ m/sec} \end{cases} \quad (16)$$

A minimum value of 10 was used with this equation to be consistent with the minimum values proposed by [Boore and Joyner \(1991\)](#) and [Cramer et al. \(2004\)](#) and with the earthquake weak motion, shallow seismic survey, and laboratory data described in the next section. Model 4 uses this same equation except that it constrains Q_{ef} to 50 when $V_S > 800$ m/sec to be consistent with Model 2.

The four Q_{ef} models are compared in Figure 4. This figure shows that Models 1 and 2 predict larger values of Q_{ef} than Models 3 and 4 for $V_S < 800$ m/sec. Model 3 predicts larger values of Q_{ef} than Model 1 for $V_S > 800$ m/sec. Models 2 and 4, which constrain the quality factor to $Q_{\text{ef}} = 50$ when $V_S > 800$ m/sec, predict larger values of Q_{ef}

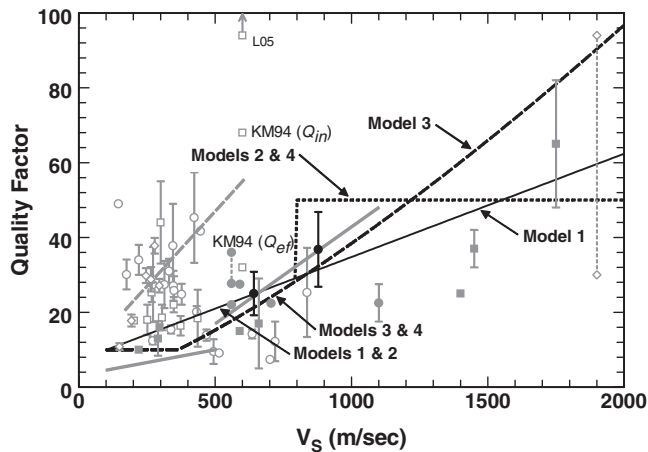


Figure 4. Comparison of the models used in this study to estimate the seismic effective quality factor Q_{ef} from the S -wave velocity V_S for sedimentary deposits (black solid and dashed lines) with values derived from earthquake weak motion, seismic survey, and laboratory data (see text): (gray solid lines) correlations derived by [Assimaki et al. \(2008\)](#) from weak-motion recordings in Japan for depth ranges of 0–30 m ($V_S < 500$ m/sec) and 30–100 m ($V_S \geq 500$ m/sec); (black solid circles) profile averages for ENA sedimentary profiles used to develop equations (20) and (22); (gray solid circles) profile averages for sedimentary profiles in ENA and Uzbekistan derived from weak-motion recordings; (gray solid squares) averages over depth intervals derived from weak-motion recordings from boreholes in California; (gray open squares) averages derived from seismic survey measurements in the Mississippi Embayment for (a) near-surface unconsolidated soils ($V_S < 500$ m/sec) and (b) the entire sedimentary column ($V_S = 600$ m/sec); (gray open circles) averages derived from seismic survey measurements in California for near-surface unconsolidated soils; (gray dashed line) relationship developed for the Mississippi Embayment from shallow refraction studies; (gray open diamonds) averages from laboratory measurements on specimens of (a) unconsolidated sediments from the Mississippi Embayment tested at confining pressures consistent with depths ranging from 2 to 30 m and (b) hard sandstone from the western United States. One standard deviation error bars are indicated when available. The error in S -wave velocity is typically smaller than the size of the symbol and is not shown. KM94, [Kang and McMechan \(1994\)](#); L05, [Langston et al. \(2005\)](#).

than Models 1 and 3 for velocities between 800 and 1200–1600 m/sec and smaller values of Q_{ef} for larger velocities. In no case is the predicted value of Q_{ef} allowed to be less than 30 when $V_S > 800$ m/sec, even though some earthquake and laboratory studies have indicated that such small values are possible. Values are allowed to exceed 50 for $V_S > 1200$ m/sec and can reach values as large as 60–100 at velocities approaching those of hard rock.

Although the four Q_{ef} models proposed in this study are loosely based on earthquake weak-motion data, they are primarily the product of the expert opinions of a few seismologists ([Boore and Joyner, 1991](#); [Cramer et al., 2004](#); [R. Herrmann and A. Akinici](#), see [Data and Resources](#) section). These seismologists give no tangible data that can be used to verify their proposed Q_{ef} profiles, so these profiles cannot be validated. There is, however, a body of weak motion, seismic survey, and laboratory data in the Mississippi Embayment, Atlantic Coastal Plain, and other sedimentary basins in California, Japan, and Uzbekistan that can be used to check whether these models are reasonable.

Weak-Motion Data

There have been several attenuation studies using weak-motion recordings in the Mississippi Embayment and the Atlantic Coastal Plain that can be used to estimate a path-averaged Q_{ef} for the sedimentary column (for details see [Dependence of Attenuation on Sediment Thickness](#) section). Two of these estimates were obtained from κ_0 values derived using the spectral-decay method ([Liu et al., 1994](#)) and the spectral-fitting method ([Chapman et al., 2003](#)). I provide an alternate estimate of Q_{ef} to that of [Liu et al. \(1994\)](#) after correcting their data for a bias inferred from the data of [Chen et al. \(1994\)](#). Two other Q_{ef} values were estimated from the ratio of the S to the converted S to P (Sp) phases ([Wuenscher et al., 1991](#); [Chen et al., 1994](#)). [Clouser and Langston \(1991\)](#) used this latter method to derive an estimate of Q_{ef} for the Gazli region of Uzbekistan. Figure 4 shows that these estimates, plotted as solid gray circles, are generally consistent with the predictions from Models 1–4. In order to show that such profile averages are a valid means of validating the Q_{ef} models, I have also plotted the values of Q_{ef} that I estimated from the sedimentary columns compiled in this study based on Q_{ef} profiles predicted from Models 1–4. These estimates also show reasonable agreement with the Q_{ef} models.

Weak-motion recordings of small earthquakes from borehole seismometer arrays can provide a direct observation of attenuation in the surrounding geologic materials if analyzed properly. However, I am not aware of any deep borehole attenuation measurements in ENA. In the absence of such measurements, I suggest that borehole recordings in California can be used as a proxy in order to gain some insight into the attenuation characteristics of similar geologic materials in ENA. There are four such studies in California. [Hauksson et al. \(1987\)](#) estimated Q_{ef} from the

uphole–downhole ratios of Fourier amplitude spectra (3–30 Hz) from recordings of a small earthquake that occurred directly beneath a deep borehole site located in the Baldwin Hills of the Los Angeles Basin. Interpreting the differences in the high-frequency slopes as due to attenuation, they estimated Q_{ef} values of 108 and 25 over depths of 0–420 m and 420–1500 m, respectively. They noted that the shallow estimates may have been overestimated due to the narrow frequency band of the data and the impact of near-surface amplification and interference. The deeper deposits were composed of upper Tertiary oil-bearing sandstones with an estimated average S -wave velocity of 1400 m/sec. Jongmans and Malin (1995) performed a similar study of Fourier spectra (2–40 Hz) using six small earthquakes located near a borehole site at Parkfield. They found Q_{ef} values of 8, 10, 65, and 37 over depths of 0–298 m, 298–572 m, 572–938 m, and 0–938 m, respectively. The two shallowest values were considered to be unreliable because of the location of the 298 m instrument in a low-velocity zone. The borehole sediments are composed of a mixture of Tertiary claystone, siltstone, sandstone, and conglomerate with average estimated S -wave velocities of 1450 m/sec for the entire borehole and 1750 m/sec for the lower section of the borehole, according to the average S -wave travel times given in Daley and McEvelly (1990). Abercrombie (1997) performed a similar study of Fourier spectra (3–30 Hz) from 17 small earthquakes located near a borehole site at Cajon Pass in the San Bernardino Mountains. She found Q_{ef} values and average S -wave velocities (in parentheses) of 17 (660 m/sec), 24 (2240 m/sec), 52 (3420 m/sec), and 25 (2090 m/sec) over depths of 0–300 m, 300–1500 m, 1500–2900 m, and 0–2900 m, respectively. The upper 300 m section of the borehole is composed of Tertiary sandstone that overlies 200 m of Tertiary sandstone and 2400 m of crystalline rock. Bonilla *et al.* (2002) used synthetic and recorded seismograms (0–10 Hz) from a small nearby earthquake in a borehole in Garner Valley (near Anza) to calibrate a near-surface velocity and damping profile that had been estimated from geotechnical data and shallow seismic surveys. Their calibration yielded Q_{ef} values and average S -wave velocities of 10 (220 m/sec), 15 (590 m/sec), 30 (1630 m/sec), and 50 (3000 m/sec) over depths of 0–22 m (Quaternary alluvium), 22–87 m (weathered granite), 87–219 m (granite), and 219–500 m (granite), respectively. The values for the sedimentary deposits and the weathered granite obtained from these borehole studies are plotted in Figure 4 (gray solid squares), where they are compared to the four Q_{ef} models proposed in this study. All of the values fall at or below the values predicted by the four models. Although not plotted, the same observation would be true for the hard-rock values. In fact, after reviewing the quality factors found by several deep borehole studies of weak-motion recordings in the frequency range of 1 to 10 Hz in California, Abercrombie (1998) concluded that these values are generally independent

of rock type and have typical values corresponding to $Q_{ef} \approx 10$ in the upper 100 m and $Q_{ef} \leq 30$ in the upper 500 m.

Assimaki *et al.* (2008) developed Q_{ef} versus V_S correlations from an inversion of uphole and downhole weak-motion geotechnical array recordings at 38 stations of the Japanese KiK-Net strong-motion network (Aoi *et al.*, 2000) from aftershocks of the 2003 M 7.0 Miyagi-oki earthquake. They used a seismic waveform optimization algorithm to derive high-resolution, low-strain estimates of Q_{ef} and V_S at the 38 KiK-Net sites from 14 aftershocks (M 4.0–4.8) located at hypocentral depths of approximately 70 km. They developed separate correlations for layers lying between sediment depths of 0–30 m and 30–100 m. The correlations for both depth ranges clearly show a near-linear relationship between Q_{ef} and V_S similar to that found in this study. Because they did not fit curves through these correlations, I estimated these curves by eye and have plotted them in Figure 4 (gray solid lines). Although there are layers below 30 m that have $V_S > 500$ m/sec, I limited the relationship to this velocity because Q_{ef} becomes relatively constant at 10 ± 5 for the higher-velocity layers, possibly reflecting a natural limit to Q_{ef} at such shallow depths. There were no layer velocities less than 500 m/sec for the 30–100 m depth range; however, I limited the upper range of the relationship to $V_S < 1100$ m/sec to be consistent with the deepest estimated velocities for the Mississippi Embayment and because, like for the shallower depths, Q_{ef} decreases to become relatively constant at about 35 ± 25 above this velocity, again possibly reflecting a natural limit for Q_{ef} in this depth range. Figure 4 shows that the two curves are generally similar to Model 3 of this study, which I derived from the Q_{ef} and V_S versus depth relationships developed for the Mississippi Embayment by R. Herrmann and A. Akinci (see Data and Resources section). The relatively small mean effective quality factors ($Q_{ef} < 10$) that were found for the soft shallow deposits are not unprecedented. Similarly small values have been found by Kudo and Shima (1970), Gibbs and Roth (1989), and Jongmans and Malin (1995).

Wald and Mori (2000) found that Q_{ef} values similar to those found by Assimaki *et al.* (2008) for Japan and Abercrombie (1998) in California could explain weak-motion site amplification data in the Los Angeles Basin. The amplification data were estimated by Hartzell *et al.* (1996, 1998) based on aftershocks of the 1994 M 6.7 Northridge earthquake. These empirical site amplifications were compared with those calculated using the propagator-matrix method of Haskell (1960) and the quarter-wavelength method of Joyner *et al.* (1981) and Boore (2003). Comparisons were made for Fourier amplitude spectra in the 1–7 Hz frequency band at 33 borehole sites where in situ S -wave velocity measurements were available. The shallow borehole data were merged with a 3D velocity model developed by Magistrale *et al.* (1996) to extend the profiles to a depth of 5 km. Wald and Mori found that the site amplifications from the weak-motion data were reasonably consistent with the site amplifications calculated from the two site-response

methods when Q_{ef} values of 10 and 30 were assigned to the depth ranges 1–100 and 100–1000 m, respectively. Although S -wave profiles were not presented, based on tabulated values of V_{S30} and a deep S -wave velocity profile presented in their paper, V_S appears to range between a few hundred meters per second near the surface to around 2000 m/sec at a depth of 1000 m. Without specific S -wave velocities, these values cannot be plotted in Figure 4. However, it is clear that they are similar to the other earthquake weak-motion estimates in this plot and would fall below the predictions from Models 1–4.

Seismic Survey Data

There have been several seismic surveys in shallow unconsolidated deposits in the Mississippi Embayment that imply that the quality factors of these deposits might be larger than is estimated by Models 1–4. These surveys were conducted using three methods: vertical seismic profiling (VSP), spectral analysis of surface waves (SASW), and seismic refraction. Pujol *et al.* (2002) and Ge *et al.* (2009) used VSP measurements from a compressed-air-driven hammer to estimate S -wave attenuation in seven shallow (approximately 60 m deep) boreholes located in the region around Memphis. Quality factors were estimated for the 10–50 Hz frequency band from the slopes of the uphole–downhole Fourier spectral ratios. Lai *et al.* (2002) used SASW to determine the spatial attenuation of Rayleigh waves produced using a vertical harmonic wave generator at a site on Mud Island near downtown Memphis. Quality factors were estimated for frequencies in the 5–70 Hz frequency band from the simultaneous inversion of surface-wave dispersion and attenuation data. Wang *et al.* (1994) used shallow refraction measurements produced with a plank and hammer at 20 sites to estimate S -wave attenuation in the region around Paducah, Kentucky. They estimated the quality factors of individual soil layers for frequencies of 0 to 40–60 Hz from critical refractions using the pulse-broadening technique. These estimates that ranged between 8 and 58 were used to develop a relationship between Q_{ef} and V_S given by the equation

$$Q_{\text{in}} = 0.08 V_S + 6.99 \quad (17)$$

for S -wave velocities ranging between 175 and 610 m/sec. The standard error of estimate of this relationship is 12.10. The inferred quality factors are assumed to represent intrinsic attenuation for reasons presented later in this section. Only the upper 30 m of the sediments investigated by Wang *et al.* (1994), representing S -wave velocities of 175–260 m/sec, are Quaternary in age (Harris and Street, 1997). The deeper and higher-velocity sediments represent Eocene or older strata. According to figure 9 of Wang *et al.* (1994), the quality factors within the Quaternary sediments range between 8 and 28, with most falling between 16 and 28. These values are similar to those found from the VSP measurements in similar age deposits. All of these estimates are plotted in Figure 4

(gray open squares and gray dashed line), where they can be compared with the predictions from Models 1–4.

Similar results to those found in the Mississippi Embayment have also been found in California using the VSP and SASW methods. Rix *et al.* (2000) applied the same surface-wave technique that Lai *et al.* (2002) used in Memphis to estimate the damping ratio $\xi = 1/2Q_{\text{in}}$ of soil layers down to a depth of 12.5 m at the Treasure Island National Geotechnical Experimentation Site in San Francisco Bay. Their damping ratios, corresponding to $\bar{Q}_{\text{in}} = 49$ for fill and soft bay mud with $\bar{V}_S = 145$ m/sec, were found to be similar to those derived from low-strain resonant column and torsional shear tests on homogenous soil specimens from a nearby borehole. The consistency between the SASW and low-strain laboratory measurements indicates that the SASW method measures primarily internal or intrinsic damping. Boore *et al.* (2003) used VSP measurements to estimate an average damping ratio of 0.012 ($\bar{Q}_{\text{in}} = 42$) in the upper 220 m of a borehole with $\bar{V}_S = 446$ m/sec located at the site of the I10 La Cienega Boulevard Bridge collapse during the 1994 Northridge earthquake. They calibrated synthetic seismograms with the observed uphole–downhole Fourier spectral ratios in order to account for the nonintrinsic attenuation resulting from geometrical attenuation, interlayer reflections and reverberations, and changes in S -wave impedance. As a result, their estimate of attenuation likely corresponds to Q_{in} rather than Q_{ef} . They also noted that this damping ratio was somewhat low compared to those that had been obtained using the same method at other shallow (10–70 m deep) borehole sites in California with comparable velocities and fine-grained soils that range between 0.014 and 0.020 ($\bar{Q}_{\text{in}} = 25$ to 36). These latter Q_{in} values along with several others that sample coarse-grained soils and soft rock (D. Boore, see Data and Resources section) are plotted along with those of Rix *et al.* (2000) and Boore *et al.* (2003) in Figure 4 (gray open circles). These values are found to fall in the same range as those in the Mississippi Embayment, and both are generally larger than those determined from weak-motion recordings. The seismic survey measurements on stiff soils and rock are the exception. These values are inexplicably smaller than those derived from weak-motion recordings for $V_S > 450$ m/sec.

The comparisons in Figure 4 show that the estimates of the quality factors in the Mississippi Embayment that were obtained from shallow seismic surveys are larger than those that were derived from earthquake weak-motion data. This is true for the predictions from Models 1–4 as well as estimates that have been derived for the entire sedimentary column (Clouser and Langston, 1991; Wuenschel *et al.*, 1991; Chen *et al.*, 1994; Liu *et al.*, 1994; Chapman *et al.*, 2003; see also Dependence of Attenuation on Sediment Thickness section) and from borehole observations presented in the previous section. Although this could imply that the earthquake estimates are too low, there is evidence to suggest that this discrepancy might instead be due to the predominant attenuation mechanism and shear-strain amplitude of the

measurements. The spectral-ratio methods that were used to derive the earthquake estimates potentially measure a combination of intrinsic and scattering attenuation. On the other hand, the seismic survey estimates in the Mississippi Embayment appear to represent primarily intrinsic attenuation because of the generation and spectral analysis of simple pulses rather than complex waveforms. For example, [Barker and Stevens \(1983\)](#) generated fundamental mode Rayleigh waves using a 1 ton soil compactor and the amplitude decay with distance to estimate the Q_{in} structure at three sites in the Imperial Valley. The S -wave velocity structure was found by simultaneously inverting the phase and group velocities. They found that Q_{in} increased from about 15–30 near the surface to 60–120 at a depth of 70 m for unconsolidated sediments with S -wave velocities ranging from 150 to 350–m/sec. These values are similar to those calculated by [Wang et al. \(1994\)](#) from the distance decay of direct arrivals of critically refracted waves. [Ge et al. \(2009\)](#) used a synthetic wave-propagation algorithm that included reverberations within layers, dispersion effects, and anelastic (intrinsic) attenuation to confirm that the estimates of attenuation that they obtained from the spectral-ratio method using VSP measurements were consistent with intrinsic attenuation. They found that they could match the amplitudes of the synthetics using their measured quality factors as estimates of Q_{in} , suggesting that scattering effects are not a significant contributor to their estimates of attenuation and, by analogy, to those of [Pujol et al. \(2002\)](#). They suggested that scattering effects are minimized because of the relatively thick layers (i.e., weak heterogeneities) within the upper 60 m of the sites that they investigated.

[Langston et al. \(2005\)](#) used the SASW method to estimate an average Q_{in} of 100 in the entire sedimentary section of the Mississippi Embayment from an analysis of the group velocity and amplitude–distance decay of band-pass-filtered explosion-generated Rayleigh waves. They interpreted the attenuation to be independent of depth and frequency in the 0.6–4 Hz frequency band. Three shallow chemical explosions of 23, 1134, and 2268 kg were used to generate Rayleigh waves out to distances as far as 130 km. Basic assumptions of the analysis were that the dominating pulses in each of the band-pass waveforms represented fundamental mode Rayleigh waves that propagated with $r^{-1/2}$ geometrical spreading and that intrinsic attenuation could be represented by a temporal rather than a spatial formulation. These assumptions were verified using synthetics. The lack of any significant contamination of the intrinsic attenuation estimates from scattering effects is also suggested by the larger value of P -wave Q_{in} ([Anderson et al., 1965](#); [Kang and McMechan, 1994](#)) that was found to be twice that of the S -wave value. [Langston et al.](#) noted that their estimate of Q_{in} is more than three times higher than the estimates of 10–30 obtained in previous investigations in the Mississippi Embayment and hypothesized that unconsolidated and semiconsolidated sediments of the embayment might not significantly attenuate low-strain earthquake ground motions, consistent with the

earlier conclusions of [Langston \(2003b\)](#). This value is large even for intrinsic attenuation and, if verified in future studies, could have a large impact on the estimated seismic hazard in the Mississippi Embayment. [Morozov \(2008\)](#) found a similar value of Q_{in} in unconsolidated and semiconsolidated sediments of 1.5 to 2 km thickness in the Kanto Plain near Tokyo from weak-motion borehole recordings reported by [Kinoshita \(2008\)](#).

[Kang and McMechan \(1994\)](#) used seismograms recorded at distances of 6 to 10 km from the shot point of a wide-aperture refraction experiment in the Mississippi Embayment in an attempt to estimate both Q_{in} and Q_{sc} . They used the common assumption that Q_{in} is relatively independent of frequency and that Q_{sc} is dependent on frequency in the frequency range of interest. They also assumed that the maximum scattering attenuation occurs at wavelengths near the dominant scatterer size that in this case was estimated to be 100 m. Simultaneous inversion of both direct P - and S -wave parameters yielded $Q_{in} = 68$ and $Q_{sc} \approx 60$ (the latter scaled from their figure 7) for the 0.8–6 Hz frequency band that gives $Q_{ef} = 32$ based on equation (2). The near equality of intrinsic and scattering attenuation demonstrates the importance of scattering effects over the 6–10 km horizontal distance used for the inversion. The value of Q_{ef} , if it represents attenuation within the entire sedimentary column, is near the upper bound of earthquake estimates within the Mississippi Embayment and the other sedimentary basins described previously. However, [Langston et al. \(2005\)](#) noted that the primary S -wave arrivals at these distances appear to represent the attenuation due to that portion of the travel path that exists within the basement rock rather than in the sediments. However, if this were the case, I would have expected the quality factors, especially Q_{in} , to be much larger. The [Kang and McMechan \(1994\)](#) and [Langston et al. \(2005\)](#) quality factors are plotted in Figure 4 (gray open squares), assuming $\bar{V}_S \approx 600$ m/sec for the sedimentary column in the Mississippi Embayment ([Andrews et al., 1985](#)).

Laboratory Data

[Chang et al. \(1992\)](#) performed resonant column tests on 35 soil specimens collected from local government agencies and engineering consulting companies in the upper Mississippi Embayment. They used these tests to estimate the low-strain and high-strain shear modulus and damping ratio for each of the specimens. Shear modulus is related to S -wave velocity through the relationship $G = \rho V_S^2$, where ρ is the density of the soil. The low-strain tests were conducted at shear-strain amplitudes of 10^{-5} and less. Tests were done at confining pressures simulating depths of a few meters up to 30 m. Soil specimens were divided into six groups depending on their soil type: A1, alluvial sand (SP-SM); A2, terrace sand and gravel (SP-SW-SM-SC-GP); A3, Jackson fine sand (SP); B1, silty to sandy clay (CL); B2, Jackson clay (CL-CH); and C, loess (fine silt). The letters in parentheses represent the soil classification based on the Unified Soil

Classification system. The tests yielded individual low-strain estimates of S -wave velocity that ranged between 100 and 480 m/sec and individual low-strain estimates of Q_{in} that ranged between 6 and 280. Although individual estimates of Q_{in} were found to vary by almost two orders of magnitude, the large number of tests provided stable mean values. These mean values along with their standard errors are plotted in Figure 4 (gray open diamonds). They generally plot in the middle of the values determined from the shallow seismic surveys and very close to the relationship derived by Wang *et al.* (1994). The exception is Jackson clay, which with $\bar{V}_S = 150$ m/sec and $\bar{Q}_{in} = 11$, had the lowest mean effective quality factor of any of the soil groups tested. This quality factor was consistent with the predictions from Models 1–4 even though it represents an estimate of intrinsic damping.

Whitman and Richart (1967) list typical values of internal (intrinsic) damping in soils from laboratory tests run at relatively small strain amplitudes ($\sim 10^{-4}$) normally encountered in foundation vibration problems and at confining pressures appropriate for near-surface soils. These values vary between 0.01 and 0.10 ($Q_{in} = 5$ to 50) with a median value of approximately 20. Clay and silty sands had the lowest values of Q_{in} , consistent with the Mississippi Embayment soil specimens, and dry and saturated sands and gravels had the highest. Although not reported, the S -wave velocities associated with these soil specimens are likely around 200 m/sec, which makes these values consistent with the laboratory values of Chang *et al.* (1992) and the values derived from shallow seismic surveys plotted in Figure 4.

Laboratory measurements of attenuation for homogeneous rock typical of embayment lithology (e.g., Gombert *et al.*, 2003) that were performed at relatively low confining pressures consistent with sediment depths in the Mississippi Embayment and the Atlantic Coastal Plain are reported to be about 10 for shale and 20–30 for sandstone for frequencies in the 20–125 Hz range (Knopoff, 1964; Lay and Wallace, 1995). Johnston and Toksoz (1980a,b) made laboratory measurements of intrinsic attenuation of S and P waves in hard sandstone ($V_S > 2000$ m/sec) at frequencies of 10–20 kHz under both low-strain and high-strain conditions. At such high frequencies, strain amplitudes are relatively high, and attenuation is increased by scattering from microfractures within the specimens. Therefore, these results are more likely a measure of Q_{ef} rather than Q_{in} . The test results of Johnston and Toksoz (1980b) for shear-strain amplitudes of 10^{-6} – 10^{-5} correspond to inferred S -wave quality factors of approximately 30–70 for dry specimens of hard sandstone, assuming that P -wave and S -wave quality factors are approximately equal (Johnston and Toksoz, 1980a). High-strain measurements of S -wave attenuation on these same specimens at large confining pressures (500–1000 bars) that presumably replicate low-strain conditions (Johnston and Toksoz, 1980a) yielded quality factors of around 30 for saturated sandstone and around 100 for dry sandstone. The range of inferred low-strain quality factors for the dry and

saturated sandstone specimens is plotted in Figure 4 (gray open diamonds connected by a gray dashed line) at an S -wave velocity of 1900 m/sec. These laboratory values are found to bracket the predictions from Models 1–4, assuming that they represent an estimate of effective rather than intrinsic attenuation. The relatively high attenuation that has been found for saturated sandstone might help to explain the relatively low quality factors that have been estimated for Mississippi Embayment and Atlantic Coastal Plain sediments from weak-motion data.

Effect of Shear-Strain Amplitude

What is referred to as low-strain shear-strain amplitude will vary depending on the method used to conduct the attenuation measurements and on the stiffness of the sediments. The low-strain asymptote of damping versus shear-strain curves from laboratory test data generally have shear-strain amplitudes of 10^{-6} and less. Low-strain seismic survey tests can induce shear-strain amplitudes as high as 10^{-5} . Low-strain weak-motion data can generate shear-strain amplitudes as high as 10^{-4} . Internal damping versus shear-strain curves from laboratory test data (e.g., Chang *et al.*, 1992; EPRI, 1993) indicate that damping can increase significantly over this range of shear-strain amplitude. For example, the EPRI curves for confining pressures consistent with depths of 0–36 m predict an increase of the damping ratio from about 0.01 at 10^{-6} shear strain to about 0.03 at 10^{-4} shear strain. This corresponds to a decrease of 70% in Q_{in} from 50 to 15. Drnevich and Richart (1970) provide a specific example based on laboratory tests on virgin specimens of dry Ottawa sand that were compacted to confining pressures consistent with depths of 6 m or less. They found damping ratios on the order of 0.005 ($Q_{in} = 100$) and 0.015 ($Q_{in} = 30$) at shear-strain amplitudes of 10^{-5} and 10^{-4} , respectively. Damping ratios were found to increase by about a factor of 2 (i.e., Q_{in} was found to decrease by a factor of 2) when the sand was subjected to a million cycles of prestrain at a shear-strain amplitude of 6×10^{-4} . These prestrained estimates are similar to those predicted by the EPRI curves for the same shear-strain amplitudes. Laboratory experiments by Johnston and Toksoz (1980b) at frequencies of 10–20 kHz provide an example of the strain-dependence of attenuation in hard rock. They found that values of P -wave Q_{in} decreased from about 60–75 at 10^{-6} compressional strain to about 30 at 10^{-5} compressional strain for two specimens of dry, hard sandstone. Silva *et al.* (1999b) also noted that stiffer materials, including rock, are just as sensitive to shear-strain amplitude as softer materials. However, because these materials are harder, higher ground-motion amplitudes are required to generate the same shear-strain amplitude. Additional discussion of the inconsistency between quality factors obtained from low-strain laboratory data and earthquake weak-motion data can be found in the Discussion and Conclusions section.

Discussion

The site attenuation parameter κ_0 , when used in conjunction with the quarter-wavelength method of site amplification defined in equation (8), must account for all attenuation mechanisms, whether they are due to intrinsic anelasticity or to scattering effects. The reason for this is that the quarter-wavelength method is based on the nonresonant amplification produced as a result of energy conservation of waves propagating through materials of gradually changing velocity (Joyner *et al.*, 1981) that ignores geometrical damping mechanisms such as geometrical attenuation, phase conversions, and scattering from reverberations between layers and from heterogeneities within the sediments. Therefore, it is altogether appropriate to estimate κ_0 using the lower values of low-strain Q_{ef} that are obtained from weak-motion data because they include the effects of both intrinsic and scattering attenuation. It also should be noted that observations of weak-motion data represent generally larger shear-strain amplitudes (up to 10^{-4}) with a correspondingly smaller Q_{ef} (possibly by a factor of 2) than low-strain seismic survey and laboratory measurements, as evidenced by the studies presented in the previous section. These higher shear-strain amplitudes are also consistent with the low-strain NEHRP site coefficients for site classes C, D, and E that attain their highest values at a relatively high peak acceleration of 0.1 g for site class B. Therefore, low strain in the context of this study refers to shear-strain amplitudes that are consistent with those induced by weak-motion recordings. Figure 4 indicates that the four Q_{ef} models proposed in this study are generally consistent with Q_{ef} values derived from weak motions. Therefore, I conclude that these models are appropriate for estimating κ_0 of sedimentary deposits for this study.

The impact of the uncertainty inherent in the four Q_{ef} models proposed in this study is demonstrated by using them to estimate κ_0 for the Memphis site profile described previously. Equation (10) yields κ_0 values of 59.1, 54.4, 74.0, and 70.2 msec for the Memphis sedimentary column using Models 1–4, respectively. These values correspond to average Q_{ef} values of 23.8, 25.8, 19.0, and 20.0. The κ_0 values bracket the value calculated from the intermediate Q_{ef} profile in Table 1 and reasonably represent the uncertainty corresponding to the Boore and Joyner (1991) and Cramer (2004) Q_{ef} profiles. Corresponding κ_0 values for the BC section of the sedimentary column are 18.0, 13.3, 17.3, and 13.5 msec for Models 1–4, respectively, yielding average Q_{ef} values of 32.9, 44.5, 34.2, and 43.8. In this case, the estimated values of κ_0 do not bracket the value calculated from the intermediate Q_{ef} profile because both the Boore and Joyner (1991) and Cramer (2004) profiles assume that $Q_{\text{ef}} = 50$ at the larger S -wave velocities; whereas, I used estimates as low as 30 for two of the Q_{ef} models. The lower estimate is consistent with many of the borehole measurements described in the previous section for unconsolidated and semiconsolidated deposits of similar or larger S -wave velocity. There is some evidence that suggests that Q_{in} might be as high as 100 in

sediments of the Mississippi Embayment (e.g., Langston *et al.*, 2005), but as I mentioned previously, it is Q_{ef} (combined intrinsic and scattering attenuation) that is relevant to the calculation of κ_0 . Therefore, for the estimates of κ_0 presented in the next section, I used Models 1–4 to estimate Q_{ef} from V_S in addition to any quality factors that were recommended by the investigator. I believe that these models adequately represent the uncertainty inherent in Q_{ef} estimates according to values reported in the literature for similar types of deposits.

Estimates of κ_0 for Sedimentary Deposits

In this section I augment the previously summarized measured values of κ_0 for sedimentary and BC sites in ENA (Table 2) with calculations using equation (10). The calculations use site profiles obtained from studies reported in the literature in order to gain an understanding of what an appropriate value or range of values might be for sedimentary and BC site profiles in ENA. The S -wave velocity and Q_{ef} profiles used for the calculations are plotted in Figures 5 and 6. The results are listed in Table 2. Following is a brief description of the studies that were used in these calculations.

Boore and Joyner (1991) developed a generic 650 m deep sedimentary column for ENA from in situ measurements of S -wave velocity summarized by Bernreuter *et al.* (1985) and Q_{ef} values inferred from weak-motion recordings in the Mississippi Embayment. The BC section of this sedimentary column is 565 m thick. Using equation (10), I calculated a κ_0 of 29.7 msec ($Q_{\text{eff}} = 27.5$) for this sedimentary column using the inferred Q_{ef} profile that agrees with the 30 msec value given in the paper. As seen in Table 2, the values of κ_0 and Q_{ef} from the inferred Q_{ef} profile fall near the high and low range, respectively, of the values calculated from the four Q_{ef} models proposed in this study. This is consistent with their assignment of $Q_{\text{ef}} = 50$ over a substantial thickness of the profile, which I used to represent one end member of the Q_{ef} models proposed in this study.

Wen and Wu (2001) developed generic S -wave velocity profiles for the cities of Memphis, Tennessee; Carbondale, Illinois; and St. Louis, Missouri, for which the depths to hard rock ($V_S > 2000$ m/sec) were estimated to be 1000, 165, and 16 m, respectively. They reported κ_0 values of 63, 43, and 7.6 msec for these three sedimentary columns that they calculated using equation (13) (C. Wu, personal comm., 2008). The sediments beneath Carbondale and St. Louis have S -wave velocities no greater than 310 m/sec and directly overly Paleozoic limestone with $V_S = 2900$ m/sec that makes them very shallow soil sites. Such sites are subject to strong resonance effects and, as a result, are unsuitable for estimating κ_0 for purposes of this study. Therefore, I limited my calculations to the Memphis sedimentary column. The BC section of this column is 600 m thick.

Park and Hashash (2004) used weak-motions recorded in the Mississippi Embayment at distances of 149–307 km from the 4 May 2001 (M 4.5) Enola, Arkansas, earthquake to

Table 2
Summary of κ_0 Values for Selected Site Profiles in ENA

Description	Site-Profile Identification			Thickness (m)					Site Attenuation Parameter κ_0 (msec)			
	Data Source	Sedimentary Column	BC Section	Method of Analysis ^a	Geological Profile ^b		BC Site Profile ^c		Sediments Only	\bar{Q}_{ef}	Including Hard Rock	Including Hard Rock
					\bar{Q}_{ef}	Including Hard Rock	\bar{Q}_{ef}	Including Hard Rock				
ENA deep soil	Boore and Joyner (1991)	650	565	2	29.7	27.5	34.7	15.4	43.7	20.4	20.4	
ENA soft rock	Silva and Darragh (1995)	-	-	5	20.6–30.5	26.7–39.6	25.6–35.5	14.2–22.1	30.4–47.4	19.2–27.1	17.0	
ENA BC site	Frankel <i>et al.</i> (1996)	-	175	1	-	-	-	12.0	-	10.0	10.0	
ENA BC site	Silva <i>et al.</i> (1999b)	-	-	5	-	-	-	3.4–4.0	37.3–43.1	8.4–9.0	8.4–9.0	
St. Louis, MO	Wen and Wu (2001)	16	-	2	-	-	12.6	-	-	-	-	
Carbondale, IL	Wen and Wu (2001)	165	-	4	43.0	-	48.0	-	-	-	-	
Memphis, TN	Wen and Wu (2001)	1000	600	4	62.7	22.3	67.7	25.7	28.6	30.7	30.7	
Summerville, SC	Chapman <i>et al.</i> (2003)	775	-	5	44.0–63.1	22.2–31.8	49.0–68.1	15.1–25.3	29.1–48.5	20.1–30.3	-	
Memphis, TN	Cramer <i>et al.</i> (2004)	960	564	1	49.0	22.4	54.0	-	-	-	-	
Mississippi Embayment (lowlands)	Park and Hashash (2004)	1010	513	2	48.2	29.1	53.2	11.9	49.5	16.9	16.9	
Mississippi Embayment (uplands)	Park and Hashash (2004)	1010	513	5	54.4–74.0	19.0–25.8	59.4–79.0	13.3–18.0	32.9–44.5	18.3–23.0	18.3–23.0	
Charleston, SC	Chapman <i>et al.</i> (2006)	830	327	3	59.6	24.8	64.6	7.8	74.2	12.8	12.8	
SRS ^d , GA	Lee <i>et al.</i> (1997, 2007)	294	116	5	55.7–73.0	20.2–26.5	60.7–78.0	13.0–18.3	31.5–44.4	18.0–23.3	18.0–23.3	

^aMethod used to estimate κ_0 : (1) estimated from recordings using the spectral decay or spectral-fitting methods; (2) equation (10) with earthquake inferred Q_{ef} values; (3) equation (10) with geotechnically inferred Q_{ef} values; (4) equation (10) with Q_{ef} values from equation (13); (5) equation (10) with Q_{ef} values from Models 1–4.

^bValues in italics were calculated by either adding or subtracting 5 msec from the values for the geological or BC site profiles (or the sedimentary column and BC section of the sedimentary column) to account for the contribution from the underlying hard rock (see text).

^cSavannah River Site

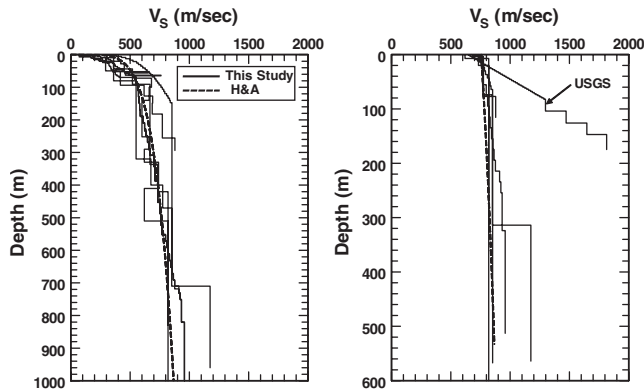


Figure 5. S -wave velocity profiles for the sedimentary columns (left) and the BC section (right) of the sedimentary columns compiled in this study (Table 2). Each profile terminates at hard rock ($V_S \geq 2000$ m/sec). H&A, the generic S -wave velocity profile for the Mississippi Embayment developed by R. Herrmann and A. Akinci (see [Data and Resources](#) section); USGS, the hypothetical BC site profile of [Frankel et al. \(1996\)](#).

back calculate a low-strain damping profile for the embayment. The recording sites were located in the lowlands (alluvium) and uplands (loess) regions of the embayment with depths to Paleozoic bedrock (hard rock) between 250 and 720 m. They used the 1010 m deep lowlands and uplands S -wave velocity profiles developed by [Romero and Rix \(2001\)](#) to define the low-strain shear modulus. The back-calculations were performed by comparing the recorded ground motions with those calculated from nonlinear site-response analyses using bedrock motions developed using the point-source stochastic simulation method. The modulus and damping curves developed by EPRI (1993) were modified to use the low-strain damping values from the back cal-

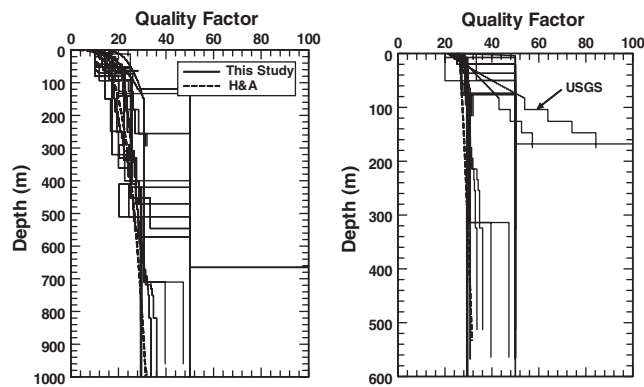


Figure 6. Q_{ef} profiles for the sedimentary columns (left) and the BC section (right) of the sedimentary columns compiled in this study (Table 2). Each profile terminates at hard rock ($V_S \geq 2000$ m/sec). The original [Park and Hashish \(2004\)](#) profile extends beyond the right boundary of the plots to a value of 125. H&A, the generic Q_{ef} profile for the Mississippi Embayment developed by R. Herrmann and A. Akinci (see [Data and Resources](#) section); USGS, the hypothetical BC site profile of [Frankel et al. \(1996\)](#) with Q_{ef} values estimated from Models 1–4 proposed in this study.

culations. As seen in Table 2, the values of κ_0 and \bar{Q}_{ef} for the sedimentary column that were estimated using the Park and Hashish back-calculated Q_{ef} profile fall within the range of values calculated from the four Q_{ef} models proposed in this study. However, the values for the BC section of the sedimentary column fall well outside of the range calculated from these four models as a result of their relatively large estimate of $Q_{ef} = 125$ for the deeper part of the profile. Additional discussion of this back-calculated Q_{ef} profile is presented later in the paper.

[Chapman et al. \(2006\)](#) used velocity measurements, shallow geotechnical studies, and geological investigations conducted by various investigators to develop 52 detailed 830 m thick S -wave velocity profiles in the Charleston area. The BC section of the sedimentary column for all of these profiles is 327 m thick. The profiles are underlain by Mesozoic and Paleozoic basement rocks of high S -wave velocity (hard rock). These authors performed site-response analyses for each of the profiles using the 1D equivalent-linear method with modulus and damping curves that were developed from laboratory measurements. Basement-rock ground motions were estimated using the point-source stochastic simulation method. They found that many of the laboratory measurements predicted very small low-strain damping ratios (in some cases equivalent to $Q_{in} > 1000$). As a result, they constrained the low-strain value of Q_{in} to be no larger than 100 for the sediments below a depth of 100 m, noting that even these values are high when viewed in comparison with most published studies of attenuation using weak-motion data from earthquakes that report values typically less than 50. For example, using a shear-strain amplitude of 10^{-6} for a typical site in downtown Charleston, the Q_{in} values assumed by [Chapman et al. \(2006\)](#) resulted in a site attenuation parameter and average quality factor of $\kappa_0 = 15$ m sec and $Q_{in} = 85$ over the 830 m thick sedimentary column that they noted is inconsistent with the $\kappa_0 = 49$ m sec that [Chapman et al. \(2003\)](#) calculated from weak-motion recordings for the nearby shallower Summerville profile. As seen in Table 2, the relatively small value of κ_0 inferred by [Chapman et al. \(2006\)](#) for the Charleston profile is outside of the range of values from the four Q_{ef} models proposed in this study. However, their use of the larger Q_{in} values is mitigated to some extent by their use of a site-response algorithm that includes wave-propagation effects. Furthermore, the purpose of their study was to estimate site amplifications for large ground motions that are controlled by the high-strain parts of the modulus and damping curves that are unaffected by the low-strain damping values. The larger κ_0 values calculated in this study for the Charleston profile as compared to the Summerville profile is due to the softer sediments that are present in downtown Charleston, where average S -wave velocities in the upper 62–83 m of the sedimentary column range from 265–310 m/sec, or nearly a factor of 2 less than those in the Summerville area ([Chapman et al., 2003](#)).

USGS Hypothetical BC Site Profile

The hypothetical ENA BC site profile used by Frankel *et al.* (1996, 2002) and Petersen *et al.* (2008) to calculate BC ground motions for the national seismic hazard maps has a shallower depth to hard rock and a steeper S -wave velocity gradient than the relatively deeper BC site profiles described in the previous section (Fig. 5). According to Frankel *et al.* (1996), the relatively steep velocity gradient was intended to be steeper than that for a typical WNA rock site. A less steep gradient was imposed below 200 m where velocities approached those corresponding to hard rock at depth. The velocities and densities were chosen with consideration given to the gross differences in the lithology and age of the rocks in ENA as compared to coastal California, where much of the borehole data comes from that can be used to constrain velocity-depth relationships. Their expectation was that ENA rocks should have higher velocities and densities than rocks in coastal California at any given depth below the surface.

Frankel *et al.* (1996) adopted a κ_0 of 10 msec to use with this hypothetical BC site profile that they attribute to studies of S waves recorded at various levels in a 300 m borehole at the U.S. Department of Energy Savannah River Site (SRS) in Aiken, Georgia (Fletcher, 1995). Fletcher did not provide any information regarding the lithology or S -wave velocity of this borehole. However, an interpretation by R. Lee (see Data and Resources section) of the S -wave velocity measurements obtained in a borehole at this same location (Lee *et al.*, 1997, 2007) yields $V_{S30} = 310$ m/sec at this site. This S -wave velocity places the SRS profile in site class D according to the NEHRP Provisions (BSSC, 2004). The BC section of the sedimentary column has a thickness of 116 m once the sediments with $V_{S30} < 760$ m/sec are stripped away. Fletcher (1995) determined a total path t^* from recordings at the surface and at a depth of 91 m in this borehole (the basement-rock instrument was not working) from four shallow earthquakes (M 1.8–3.6) located at distances of 19–141 km from the SRS. According to the interpreted velocity log provided by R. Lee (see Data and Resources section), the S -wave velocity at the 91 m depth is estimated to be 420 m/sec, representing the lower range of NEHRP site class C, which is still significantly less than that corresponding to BC site conditions. Assuming $\kappa = t^*$, Fletcher (1995) interpreted the observed systematic increase in t^* with distance in terms of equation (7) and found a κ_0 of 6 msec for both the surface and downhole recordings. In contrast, he calculated a t^* of 14 msec from the high-frequency fall-off of the spectral ratio (surface/325 m downhole) of ground motions recorded from a blast set off near the borehole site. The similarity of the surface and downhole estimates of κ_0 from the earthquake recordings and their discrepancy with respect to the t^* inferred from the blast data lead Fletcher (1995) to dismiss the κ_0 estimates from the earthquake recordings as mostly random error.

The hypothetical USGS profile attains an S -wave velocity in excess of 2000 m/sec (hard rock) at a depth of 175 m.

The Memphis, Mississippi Embayment, and Charleston BC site profiles compiled in this study reach this velocity at depths ranging from 327 to 600 m (Table 2). The Carbondale profile of Wen and Wu (2001) has about the same depth to hard rock as the hypothetical USGS profile, but it is composed of much softer deposits in the upper 30 m and as a result has a substantially higher κ_0 of 43 msec. Without having a reasonable in situ analog for the hypothetical USGS BC site profile, I decided to derive an independent estimate of κ_0 using the same method I used to estimate κ_0 for the other BC site profiles analyzed in this study. The results are summarized in Table 2. The calculated values of κ_0 from the four Q_{ef} models proposed in this study were found to range between 3.4 and 4.0 msec ($Q_{ef} = 37.3$ to 43.1) for the BC section of the sedimentary column and between 8.4 and 9.0 msec for the entire BC site profile. These values are somewhat less than the 5 msec value ($Q_{ef} = 29.7$) for the sediments and the 10 msec value for the BC site profile assumed by Frankel *et al.* (1996).

Additional support for the relatively small κ_0 used by the USGS comes from an independent evaluation of the SRS seismic survey data. The SRS site is located northwest of Charleston where the Atlantic Coastal Plain sediments are much thinner than at Charleston or Memphis. The interpreted S -wave velocity profile for the site provided by R. Lee (see Data and Resources section) and described in Lee *et al.* (1997, 2007) indicates a depth of 294 m to hard rock. The BC section of this profile is 116 m thick, less than that assumed in the USGS profile. The range of κ_0 values for the SRS sedimentary column determined in this study (25.6–36.2 msec) is larger than the $t^* = 14$ m sec determined by Fletcher (1995) from blast data, possibly reflecting the larger shear-strain amplitudes associated with the earthquake-based Q_{ef} models proposed in this study. The values of κ_0 for the BC site profile at SRS were found to range from 9.4 to 10.1 msec (Table 2). Therefore, it appears that although there is an equivocal basis for the original value of κ_0 used to characterize site attenuation in the hypothetical USGS BC site profile (Fletcher, 1995), the selected value is relatively consistent with estimates determined from an independent assessment of κ_0 using the approach proposed in this study. Nevertheless, the issue, discussed in detail later in the article, is whether such a shallow BC site profile should be used to represent a generic BC site in ENA for hazard mapping and other seismological and engineering applications.

Dependence of Attenuation on Sediment Thickness

The estimates of κ_0 determined in this study are summarized in Table 2. The estimates for the geological and BC site profiles listed in this table are clearly dependent on the thickness of the sediments. As noted previously, Liu *et al.* (1994) also found κ_0 to be dependent on sediment thickness in the upper Mississippi Embayment. Their derived dependence of κ_0 on sediment thickness, after adding the

5 msec attributable to the hard-rock section of the geological profile, is given by the equation (Liu *et al.*, 1994)

$$\kappa_0 = 5.0 + 0.0499H_{\text{Sed}}, \quad (18)$$

where κ_0 is the site attenuation parameter for the geological profile (msec), and H_{Sed} is the thickness of the sedimentary column (m). The standard error of regression is 6.2 msec, and the standard error of the slope is 0.0019 msec/m.

Interpreting the sediments as a uniform layer over a half-space following the approach of Hough *et al.* (1988), Liu *et al.* (1994) noted that the average quality factor for these sediments could be calculated from the expression

$$\bar{Q}_{\text{ef}} = b^{-1} \bar{V}_S^{-1}, \quad (19)$$

where b is the slope of the relationship between κ_0 and H_{Sed} , and \bar{V}_S is the time-averaged S -wave velocity of the sediments. Combining this expression with equation (11), these authors calculated $\bar{Q}_{\text{ef}} = 36$, from which I calculated $\kappa_0 = 32$ msec using their estimates of $\bar{V}_S = 560$ m/sec and $\bar{H}_{\text{Sed}} = 650$ m for the PANDA stations. These latter values were derived from the difference between the S and the converted S -to- P (Sp) phase travel times and sediment thicknesses beneath each of the stations, assuming that the converted phases were generated at the base of the embayment sediments. They also calculated the differential values of the κ_0 of S and P waves from the slopes of the logarithmic Sp -to- S Fourier spectral ratios for the 4–25 Hz frequency band following the approach of Clouser and Langston (1991). They concluded that these differential values were consistent with the differences calculated using the independently derived S - and P -wave κ_0 values obtained from the spectral decay method. However, close inspection of their Figure 7 indicates that the κ_0 differences from the Sp/S ratios are systematically larger by ~ 10 msec for $\kappa_0 < 25$ msec, owing to the presence of several very small or negative differences derived from the spectral decay method. A similar discrepancy was found in the values calculated using Sp/S ratios by Chen *et al.* (1994) as discussed in the following paragraph. Liu *et al.* (1994) also applied the technique of Anderson and Humphrey (1991) to simultaneously derive both κ and the corner frequency of the ω -square source spectrum for five S -wave spectra recorded at hypocentral distances of 10–18 km from one of the events. Because of the short distances, they found that the κ values calculated from these spectra using the spectral decay method were similar to the κ_0 values obtained for the same stations using the same method. They further found that the κ values were similar between the spectral decay and spectral-fitting methods, providing additional confidence in the former, although this comparison is too limited to be considered a formal validation of the results.

Chen *et al.* (1994) analyzed more than 260 earthquakes recorded at the same PANDA stations analyzed by Liu *et al.* (1994) to estimate $Q_P - Q_S$ relations for the upper Missis-

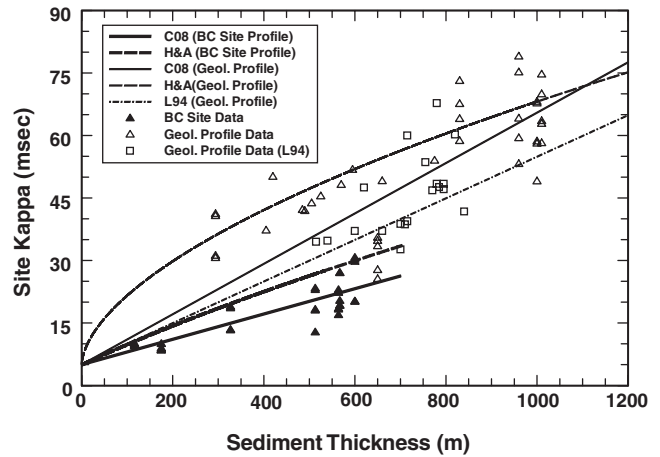


Figure 7. Relationship between sediment thickness and the site attenuation parameter κ_0 for the geological and BC site profiles compiled in this study (Table 2). The values of κ_0 for the sedimentary sections of these profiles can be determined by subtracting 5 msec from the value of κ_0 obtained from the plot. R. Herrmann and A. Akinci (H&A) (see Data and Resources section); L94, estimates from Liu *et al.* (1994) after adjusting for an apparent bias in κ_0 (see text).

issippi Embayment, where Q_P and Q_S are the frequency-independent quality factors of P and S waves, respectively. The relations were derived using Sp/S spectral ratios for a fixed frequency range of 2–25 Hz. They interpreted their average $Q_P - Q_S$ relation to infer a Q_S (\bar{Q}_{ef}) of 25 to 30, based on the assumption that Q_S falls between $0.53Q_P$ and $1.79Q_P$ as suggested by Wuenscher *et al.* (1991). The $\bar{Q}_{\text{ef}} = 36$ found by Liu *et al.* (1994) using the spectral decay method is 31% higher than the $\bar{Q}_{\text{ef}} = 27.5$ determined by Chen *et al.* (1994) using the Sp/S spectral-ratio method. This difference corresponds to an equivalent difference in the estimated value of κ_0 according to equation (11), assuming all remaining parameters are held constant. Liu *et al.* (1994) attributed this difference to the use by Chen *et al.* (1994) of a fixed lower-bound frequency of 2 Hz, which they claim is below the corner frequency of many of the smaller events used in the analysis and, therefore, can lead to a potential underestimate of the spectral slopes and resulting differential κ_0 values. However, according to the methodology used by Chen *et al.* (1994), a smaller differential κ_0 corresponds to a larger Q_S/Q_P ratio that in turn leads to a larger value of Q_S according to their figure 8. Therefore, I suggest that Chen *et al.* (1994) might have actually overestimated Q_S . This conclusion is also supported by the \bar{Q}_{ef} of 22 determined for the upper 600 m of upper Mississippi Embayment sediments by Wuenscher *et al.* (1991) using the spectral decay technique of Anderson and Hough (1984).

Following Liu *et al.* (1994), I used the κ_0 values listed in Table 2 to develop a linear relationship between κ_0 and H_{Sed} . I augmented these values with those reported by Liu *et al.* (1994) after making an adjustment to remove the apparent bias in their estimated values of \bar{Q}_{ef} based on the results of

Chen *et al.* (1994) that suggest the κ_0 values reported by Liu *et al.* (1994) might be underestimated by a factor of about 1.3 (the ratio between \bar{Q}_{ef} values of 36.0 and 27.5, the average of the range reported by Chen *et al.* (1994)). A similar bias of about 1.5 was reported by Liu *et al.* (1994) between their estimates and those from low-amplitude recordings at two strong-motion stations for which an independent estimate of κ_0 was derived by spectral fitting. I also updated the sediment thicknesses of the PANDA stations with those interpolated from well logs by Chen *et al.* (1996). A least-squares regression on these two parameters yielded the equations

$$\kappa_0 = 5.0 + 0.0605H_{\text{Sed}}, \quad (20)$$

$$H_{\text{Sed}} = 15.8 (\kappa_0 - 5.0), \quad (21)$$

where κ_0 is the site attenuation parameter of the geological profile (msec) and H_{Sed} is the thickness of the sedimentary column (m). The standard error of regression, R-square value, and standard error of the slope is 10.0 msec, 0.96, and 0.0017 msec/m for equation (20) and 161 m, 0.96, and 0.5 m/msec for equation (21). I used the average values of κ_0 and H_{Sed} for the two Park and Hashash (2004) site profiles so as not to give them undue weight in the analysis. Equation (19) yields $\bar{Q}_{\text{ef}} = 25.7$ for $b = 0.0605$ msec/m and $\bar{V}_S = 642$ m/sec, the time-averaged estimate of S -wave velocity calculated from the data used in the regression. This value is virtually identical to the $\bar{Q}_{\text{ef}} = 25.0$ obtained by averaging the observed values of Q_{ef}^{-1} . The estimates of κ_0 from both equations (18) and (20) should be decreased by 5 msec to represent the site attenuation corresponding to the sedimentary column. The median predictions from equations (18) and (20) are plotted in Figure 7, where they are compared with the relationship between κ_0 and H_{Sed} inferred from equations (13) and (15) (R. Herrmann and A. Akinci, see Data and Resources section). This figure indicates that the adjusted values of κ_0 from Liu *et al.* (1994) are in general agreement with the depth-dependence of the κ_0 values estimated in this study.

I developed a similar relationship between site attenuation and sediment thickness for the BC site data in Table 2. A least-squares regression between these two parameters yielded the equations

$$\kappa_0 = 5.0 + 0.0304H_{\text{BC}}, \quad (22)$$

$$H_{\text{BC}} = 30.8 (\kappa_0 - 5.0), \quad (23)$$

where κ_0 is the site attenuation parameter for the BC site profile (msec), and H_{BC} is the thickness of the BC section of the sedimentary column (m). The standard error of regression, R-square value, and standard error of the slope is 3.7 msec, 0.96, and 0.0014 msec/m for equation (22) and 116 m, 0.94, and 1.4 m/msec for equation (23). I used only one set of values for κ_0 and H_{BC} for the two Park and

Hashash (2004) site profiles so as not to give them undue weight in the analysis. Equation (19) yields $\bar{Q}_{\text{ef}} = 37.5$ for $b = 0.0304$ msec/m and $\bar{V}_S = 878$ m/sec, the time-averaged estimate of S -wave velocity calculated from the data used in the regression. This value is virtually identical to the $\bar{Q}_{\text{ef}} = 36.8$ obtained by averaging the observed values of Q_{ef}^{-1} . The estimates of κ_0 from equation (22) should be decreased by 5 msec to represent the site attenuation corresponding to the BC section of the sedimentary column. The median prediction from equation (22) is plotted in Figure 7.

Interpretation of Results

All of the κ_0 values for the BC site profiles listed in Table 2 fall within the two standard-error bounds of equation (22) except those estimated from the Park and Hashash (2004) site profiles using Q_{ef} values back-calculated from weak-motion data. The reason for this discrepancy is their relatively large average quality factor ($\bar{Q}_{\text{ef}} = 74.2$) that is nearly a factor of 2 higher than the estimates of 27.3–48.5 found for the other profiles compiled in this study. This is due to their estimate of $Q_{\text{ef}} = 125$ for depths below 665 m ($V_S > 850$ m/sec), which is significantly larger than the maximum value of 50 used in this study for deposits of similar S -wave velocity. In fact, it is even larger than the low-strain ($< 10^{-6}$ shear-strain) value of 83 that was determined for these same depths from laboratory tests (EPRI, 1993). Despite the relatively high value of \bar{Q}_{ef} found for the BC section of the sedimentary column, the Park and Hashash κ_0 and \bar{Q}_{ef} estimates for the sedimentary column are generally consistent with those for the other sedimentary columns compiled in this study. This is due to their lower estimates of Q_{ef} at intermediate depths within the sedimentary column as compared to the four Q_{ef} models proposed in this study. There is likely to be a trade-off between the values of Q_{ef} at intermediate depths and those at greater depths that are not easily resolved from surface recordings (Y. Hashash, personal comm., 2008). Because the back-calculated damping ratios were derived from 1D site-response analyses, it is also possible that the damping ratios at large depths within the profile were not well constrained considering that overall site response is most sensitive to amplification and attenuation in the upper 100 m of the profile (e.g., EPRI, 1993; Kramer, 1996; Silva *et al.*, 1999a,b; Langston, 2003a). This points out an important source of uncertainty in the estimates of κ_0 summarized in Table 2.

Another issue brought up by the Park and Hashash (2004) study is the discrepancy between the low-strain damping ratios back-calculated from weak-motion recordings and the low-strain damping ratios obtained from laboratory tests. These authors found that the back-calculated values of the damping ratio at shallow-to-intermediate depths within their profile were significantly larger than the low-strain damping ratios estimated from the depth-adjusted laboratory damping curves (EPRI, 1993). The low-strain

(10^{-6} shear-strain) laboratory measurements infer a Q_{in} value of 36 in the relatively soft near-surface sediments. The laboratory based values then increase rapidly to 50 at a depth of 14 m and 83 at a depth of 155 m. These values are substantially larger than those derived from weak-motion data for sediments of similar S -wave velocity in the Mississippi Embayment as well as elsewhere in the United States, Uzbekistan, and Japan (Hauksson *et al.*, 1987; Clouser and Langston, 1991; Wuenscher *et al.*, 1991; Chen *et al.*, 1994; Liu *et al.*, 1994; Abercrombie, 1997; Chapman *et al.*, 2003; Langston, 2003a,b; Assimaki *et al.*, 2008; see also the compilations in Abercrombie, 1997; Langston *et al.*, 2005). As noted previously, the likely reason for these differences are the scattering effects and the larger shear-strain amplitudes associated with the weak-motion recordings. Chapman *et al.* (2006) found a similar discrepancy in the Charleston geotechnical data and chose to restrict the low-strain values of Q_{in} obtained from laboratory tests to 100 at depths below 100 m after they found that some of these values exceeded 1000, which they considered to be inconsistent with earthquake observations. Assimaki *et al.* (2008) found a similar discrepancy between low-strain damping ratios obtained from published laboratory tests (corresponding to $Q_{in} = 15$ to 50) and those obtained from downhole recordings of the 2003 M 7.0 Miyagi-oki aftershock sequence at depths less than 30 m (corresponding to $Q_{ef} = 5$ to 20). I also found a similar discrepancy in the low-strain damping ratios obtained from laboratory tests of soil specimens from the SRS borehole (Lee *et al.*, 1997, 2007). The laboratory measurements infer Q_{in} values that range between 40 and 80 in the relatively soft near-surface sediments above 100 m and values that range between 50 and 100 for the stiffer sediments at depths between 100–300 m. On the other hand, effective quality factors at SRS estimated from the Q_{ef} models proposed in this study were found to range from 16–25 for the shallower depths and 17–50 for the larger depths.

The discrepancy between estimates of Q_{in} obtained from laboratory tests and the quality factors derived from earthquake recordings has long been recognized (e.g., Redpath *et al.*, 1982; Redpath and Lee, 1986). Redpath and Lee (1986) found a frequency-independent Q_{ef} of 13 from Fourier spectral ratios of low-strain earthquake data between depths of 15.7 and 43.7 m in a borehole in soft bay mud near Richmond, California, for which $\bar{V}_S = 290$ m/sec. In contrast, Q_{in} was found to be 20 from laboratory tests on two soil specimens from this same borehole. The spectral ratios using the surface recordings gave conflicting results, possibly due to noise contamination or a poor constraint on the amount of attenuation in the upper 6.1 m.

As noted previously, Langston *et al.* (2005) found a frequency and depth-independent Q_{in} of 100 in the Mississippi Embayment based on an analysis of the group velocity and amplitude-distance-decay of blast-generated Rayleigh waves. Morozov (2008) found a similar value using weak-motion recordings from a borehole in sediments several kilometers thick in Japan. Although this estimate represents

intrinsic rather than effective attenuation, it is useful to show what impact this larger value would have on κ_0 . Assuming $Q_{ef} = Q_{in} = 100$ with the embayment sediment thicknesses and S -wave velocity profiles given in Boore and Joyner (1991), Romero and Rix (2001), and Cramer *et al.* (2004), I calculated a κ_0 that ranged between 8 and 15 msec, substantially lower than the 21–74 msec values calculated from the Q_{ef} models proposed in this study. Langston (2003a,b) showed that the Sp/S spectral-ratio method, the basis of many of the previous Q_{ef} estimates in the embayment (Chen *et al.*, 1994; Liu *et al.*, 1994), is insensitive to intrinsic attenuation (anelasticity) because of significant near-surface site resonance effects that can amplify rather than attenuate low-strain high-frequency ground motion through the embayment sediments. However, Langston (2003b) notes that wave scattering in the embayment sedimentary column can produce a general spectral fall-off with frequency (Q_{ef}) that mimics the spectral fall-off associated with low values of Q_{in} . Assimaki *et al.* (2008) also found that attenuation due to scattering was a significant part of the total attenuation in their analysis of the 2003 M 7.0 Miyagi-oki aftershock recordings, which they suggested might be one of the causes of the discrepancy between their low-strain earthquake and laboratory damping values.

As discussed previously, the site attenuation parameter κ_0 , when used in conjunction with site amplification factors based on the quarter-wavelength method given by equation (8), must account for all attenuation mechanisms, whether they are due to intrinsic anelasticity or scattering effects. Therefore, it is entirely appropriate to use the lower values of Q_{ef} that include the effects of both intrinsic anelasticity and scattering effects when estimating κ_0 for purposes of incorporating site amplification and site attenuation in the stochastic simulation of ground motion using the quarter-wavelength method.

Discussion and Conclusions

The estimates of κ_0 calculated for the sedimentary sites in this study (Table 2) were generally found to increase linearly with the thickness of the sediments with κ_0 values for the sedimentary column ranging from as low as 8 msec for a 16 m thick column to as high as 74 msec for a 960 m thick column and values for the BC section of the sedimentary column ranging from as low as 4 msec for a 116 m thick column to as high as 26 msec for a 600 m thick column. Path-averaged estimates of Q_{ef} were found to range from 19 to 40 for the sedimentary column and from 28 to 74 for the BC section of the sedimentary column. The corresponding values of κ_0 for the BC site-profile, which include the 5 msec contribution from the hard-rock ($V_S \geq 2000$ m/sec) section of the profile that underlies the sediments, were found to range from 13 to 79 msec for the sedimentary column and from 9 to 31 msec for the BC section of the sedimentary column. These estimates are based on measurements of weak-motion recordings at sedimentary and NEHRP BC sites in ENA and on

calculations from S-wave velocity and Q_{ef} profiles that are based on weak-motion recordings in the Mississippi Embayment and the Atlantic Coastal Plain. The 17 msec value of κ_0 that was found by [Silva and Darragh \(1995\)](#) for deep soft-rock sites in ENA and the 20 msec value that was recommended by [Silva et al. \(1999b\)](#) for a generic deep BC site in ENA correspond to BC sediment thicknesses of about 370 ± 116 m and 460 ± 116 m, respectively, based on equation (23). This and a similar depth dependence found for the entire sedimentary column is consistent with the results of [Liu et al. \(1994\)](#), [Silva et al. \(1999b\)](#), and [Wen and Wu \(2001\)](#), who found that thinner sedimentary deposits correspond to smaller values of κ_0 .

The strong dependence of κ_0 on sediment thickness suggests that it might be necessary to use more than one BC site profile for seismic hazard mapping and other seismological and engineering applications that are intended to provide ground motions for a generic reference BC site condition. [Silva et al. \(1999a,b\)](#) came to a similar conclusion after conducting site-response analyses for typical site profiles of varying depths in ENA and WNA. The single ENA BC site profile currently being used by the USGS for this purpose is relatively shallow with a site attenuation parameter that falls toward the lower end of the values estimated in this study. Adopting such a regional approach to defining variable reference site conditions would likely require a similar regionalization of the low-strain NEHRP site coefficients because site amplification has also been shown to be strongly dependent on sediment thickness ([Kanai, 1983](#); [Savy et al., 1987](#); [EPRI, 1993](#); [Kramer, 1996](#); [Silva et al., 1999a,b](#)). An alternative approach would be to use hard rock as the reference site condition in ENA and develop a set of low-strain site coefficients that take into account the variability of sediment thickness and V_{S30} throughout the region.

Until a regionalized site-response model is developed, the hypothetical USGS BC site profile remains the only publicly available profile that one can use to estimate ground motions for BC site conditions in ENA. It also continues

to be the basis for the reference site condition in the 2008 national seismic hazard maps ([Petersen et al., 2008](#)). The issue then becomes what value of κ_0 should be used with this profile. The most common use of the USGS profile is to provide an estimate of BC ground motions to use in conjunction with the NEHRP site coefficients (e.g., [BSSC, 2004](#); [ASCE, 2006](#); [ICC, 2006](#)). Therefore, one way of choosing an appropriate value for κ_0 is to compare the amplification factors predicted from the USGS profile using candidate values of κ_0 with the low-strain BC site coefficients used in the building codes. I did this by first calculating Fourier spectra amplification factors from equation (8) using the USGS BC site profile and alternative κ_0 values of 10 and 20 msec with the computer program, SITE_AMP ([Boore, 1996](#)). Using these amplification factors, I then calculated 5% damped response spectral acceleration using the stochastic ground-motion simulation computer program, FAS_DRVR ([Boore, 1996](#)). This is the same method that [Frankel et al. \(1996\)](#) used to develop the amplification factors used by the USGS to estimate ground motions for BC site conditions from those on hard rock. Table 3 compares these estimates with the low-strain NEHRP short-period site coefficient F_a and the low-strain NEHRP long-period site coefficient F_v . Also listed in this table are the low-strain amplification factors used by the USGS ([Frankel et al., 1996, 2002](#); [Petersen et al., 2008](#)) and those developed by [Hwang et al. \(1997\)](#) and [Silva et al. \(1999b\)](#) for typical site profiles in ENA. The NEHRP site coefficients, the amplification factors of [Silva et al. \(1999b\)](#), and one set of the amplification factors estimated in this study are an average over periods of 0.1–0.5 sec (short-period factor) and 0.4–2.0 sec (long-period factor). The other amplification factors in Table 3 were derived for periods of 0.2 and 1.0 sec to represent the short-period and long-period spectral ranges, respectively. The NEHRP BC site coefficients and the amplification factors reported for [Hwang et al. \(1997\)](#) and [Silva et al. \(1999b\)](#) are the geometric mean of the factors for NEHRP site classes B and C.

Table 3
Comparison of Low-Strain Site Amplification Factors for BC Site Profiles in ENA*

Source	Profile Depth (m)	Short-Period Factor (0.1–0.5 sec)	Long-Period Factor (0.4–2.0 sec)
NEHRP (BSSC, 2004) [†]	-	1.37	1.63
USGS (Frankel et al., 1996) [‡]	175	1.53	1.34
Hwang et al. (1997) [‡]	300–400	1.48 (1.35, 1.63)	1.48 (1.35, 1.63)
Silva et al. (1999b) [‡]	30–300	1.50 (1.36, 1.65)	1.39 (1.26, 1.53)
This study ($\kappa_0 = 10$ msec) [†]	175	1.52 (1.38, 1.67)	1.38 (1.25, 1.52)
This study ($\kappa_0 = 20$ msec) [†]	175	1.32 (1.20, 1.45)	1.32 (1.20, 1.45)
This study ($\kappa_0 = 10$ msec) [‡]	175	1.53 (1.39, 1.68)	1.33 (1.21, 1.46)
This study ($\kappa_0 = 20$ msec) [‡]	175	1.32 (1.20, 1.45)	1.38 (1.25, 1.52)

*Note: Amplification factors are calculated with respect to ENA hard rock (NEHRP site class A). Amplification factors estimated by the USGS and in this study were calculated directly for BC site conditions; all other estimates represent the geometric mean amplification factors for NEHRP B and NEHRP C site conditions. The values given in parentheses represent a 10% uncertainty in the mean estimate, which is the estimated standard deviation of this estimate ([Silva et al., 1999b](#)).

[†]Amplification factors are an average over periods of 0.1–0.5 sec (short period) and 0.4–2.0 sec (long period).

[‡]Amplification factors are for individual periods of 0.2 sec (short period) and 1.0 sec (long period).

The results in Table 3 indicate that the low-strain NEHRP short-period site coefficients are similar to the low-strain BC amplification factors calculated in this study using $\kappa_0 = 20$ msec. As expected, the USGS short-period amplification factor is more consistent with the amplification factor calculated in this study for an individual period of 0.2 sec and $\kappa_0 = 10$ msec. The Hwang *et al.* (1997) and Silva *et al.* (1999b) short-period amplification factors are larger than those in this study, consistent with the larger depths to hard rock and the larger impedance contrast at the base of the sediments in their NEHRP site class B and C site profiles as compared to the USGS profile (Table 3). I conclude from these results that the low-strain NEHRP short-period site coefficients are most consistent with the amplification factors calculated from the USGS BC site profile when site amplification is calculated with the quarter-wavelength method using $\kappa_0 = 20$ m sec.

The results in Table 3 indicate that the low-strain NEHRP long-period site coefficients are larger than all of the other amplification factors listed in this table. As expected, the USGS amplification factor is found to be consistent with the amplification factor calculated in this study for an individual period of 1.0 sec and $\kappa_0 = 10$ msec. The discrepancy between the low-strain NEHRP site coefficients and the other long-period amplification factors suggests that there might be a systematic bias in the site coefficients when compared to the amplification factors derived from site profiles more typical of unconsolidated and semiconsolidated sites in ENA. This bias is not likely to be caused by differences in site attenuation because the value of κ_0 does not have a large influence on the one-second spectral acceleration or the Fourier amplitude spectrum as demonstrated in Table 3 and Figure 1. Instead, it likely corresponds to a WNA BC site profile that is generally thicker with a lower velocity gradient than the typical BC site profile in ENA (e.g., Boore and Joyner, 1997). I also note that the two sets of amplification factors that are the closest to the low-strain NEHRP long-period site coefficients are those that are based on the thickest site profiles (Hwang *et al.*, 1997; Silva *et al.*, 1999b), which are substantially thicker than the 175 m thick USGS profile. Because of the large disparity amongst the long-period amplification factors in Table 3, the apparent bias associated with the low-strain NEHRP long-period site coefficients and the relative insensitivity of the long-period amplification factors to the value of κ_0 , I conclude that the long-period results given in Table 3 cannot be used as a basis for selecting one value of κ_0 over another. These results also suggest that the low-strain NEHRP long-period site coefficients are not consistent with the expected amplification from the relatively shallow USGS BC site profile regardless of whether a κ_0 of 10 or 20 msec is used to define site attenuation.

Based on the results of this study and the discussion presented in the previous paragraphs, I conclude that it is more reasonable to use a site attenuation parameter or κ_0 of 20 msec rather than 10 msec with the relatively shallow hypothetical USGS BC site profile of Frankel *et al.* (1996)

for purposes of estimating ground motions that are intended to be consistent with the reference site conditions used in the national seismic hazard maps and the short-period low-strain site coefficients in the NEHRP Provisions. Although there is a large degree of uncertainty in this estimate, it is consistent with the value recommended by Silva *et al.* (1999b) for a generic NEHRP BC site in ENA and with both measured and calculated values of κ_0 for BC sites located in the Mississippi Embayment, the Atlantic Coastal Plain, the Gulf Coast region, and the Denver Basin (this study; Silva *et al.*, 1999b). This conclusion should not be interpreted to imply that the smaller κ_0 value used by the USGS is inappropriate for their relatively shallow site profile (in fact the results of this study suggest otherwise). It implies only that the use of the larger value of κ_0 provides site amplification factors that are more consistent with the low-strain NEHRP short-period site coefficients that are often used to adjust BC ground motions to site conditions representing NEHRP site classes A through E (Borcherdt, 1994; Dobry *et al.*, 2000; ASCE, 2006; BSSC, 2004; ICC, 2006). However, neither of these κ_0 values produce amplification factors that are consistent with the low-strain NEHRP long-period site coefficients, suggesting that a thicker profile would be needed in addition to a higher value of κ_0 in order to match both the short-period and long-period site coefficients.

The studies of Hwang *et al.* (1997) and Silva *et al.* (1999b) suggest that site amplification factors are likely to be different for sites with the same generic NEHRP site class in ENA and WNA due to systematic differences in lithology and tectonic environment. Furthermore, there are large areas in ENA (and to a lesser extent in WNA) where there are relatively shallow soft sediments directly overlying bedrock, corresponding to a large impedance contrast, and relatively shallow weathered rock over hard rock, corresponding to a strong velocity gradient, that do not fit easily into one of the generic NEHRP site classes defined in the building codes. These problematic site conditions require special study and further indicate that a one-type-fits-all site coefficient might not be a reasonable means of incorporating local site conditions in the development of design ground motions.

The limited review of attenuation studies presented in this article has shown that there is a large degree of uncertainty and confusion that exists with regard to the low-strain attenuation characteristics of unconsolidated and semiconsolidated sediments in ENA. This is caused by a general lack of consensus regarding the dependence of attenuation on such factors as the attenuation mechanism, sediment thickness, degree of sediment saturation, wave frequency, shear-strain amplitude, measurement methods, and calculation methods. All of these issues are being addressed in a 5 yr (2008–2012) study managed by the Pacific Earthquake Engineering Research Center, University of California, Berkeley, titled Next Generation Attenuation Models for Central and Eastern North America. This study should go a long way in starting a dialogue with the ultimate goal of developing a scientific consensus regarding these important issues.

Data and Resources

The quality factor and S -wave velocity versus depth relationships for the Mississippi Embayment attributed to R. Herrmann and A. Akinci were obtained from the Mid-America Ground-Motion Models Web page, Department of Earth and Atmospheric Sciences, St. Louis University, Missouri, at www.eas.slu.edu/People/RBHerrmann/MAEC/maecgnd.html (last accessed December 2008). An unpublished compilation of quality factors and S -wave velocities from shallow seismic surveys in California by James Gibbs, David Boore, and William Joyner was provided by David Boore of the U.S. Geological Survey (USGS), Menlo Park, California. A digital version of the S -wave velocity log for the Savannah River Site (SRS) was provided by Richard Lee of the Los Alamos National Laboratory, Los Alamos, New Mexico. A digital version of the S -wave velocity and damping logs for the Mississippi Embayment was provided by Youssef Hashash of the Department of Civil and Environmental Engineering, University of Illinois, Urbana-Champaign.

Acknowledgments

This research was supported in part by the U.S. Geological Survey (USGS) Department of the Interior under award number 05HQGR0032. The views and conclusions contained in this document are those of the author and should not be interpreted as necessarily representing the official policies, either expressed or implied, of the U.S. government. This research benefited from helpful discussions with David Boore, Martin Chapman, Youssef Hashash, Richard Lee, and Chiun-Lin Wu. I also want to thank Gail Atkinson, David Boore, and Martin Chapman for their constructive reviews that led to significant improvement of the manuscript.

References

- Abercrombie, R. A. (1997). Near-surface attenuation and site effects from comparison of surface and deep borehole recordings, *Bull. Seismol. Soc. Am.* **87**, 731–744.
- Abercrombie, R. E. (1998). A summary of attenuation measurements from borehole recordings of earthquakes: The 10 Hz transition problem, *Pure Appl. Geophys.* **153**, 475–487.
- Aki, K. (1980). Scattering and attenuation of shear waves in the lithosphere, *J. Geophys. Res.* **85**, 6496–6504.
- Aki, K., and B. Chouet (1975). Origin of coda waves: Source, attenuation, and scattering effects, *J. Geophys. Res.* **80**, 3322–3342.
- American Society of Civil Engineers (ASCE) (2006). Minimum design loads for buildings and other structures, Rept. No. ASCE/SEI 7-05, Reston, Virginia.
- Anderson, D. L., A. Ben-Menahem, and C. B. Archambeau (1965). Attenuation of seismic energy in the upper mantle, *J. Geophys. Res.* **70**, 1441–1445.
- Anderson, J. G. (1986). Implication of attenuation for studies of the earthquake source, in *Earthquake Source Mechanics*, S. Das, J. Boatwright, and C. H. Scholz (Editors), Maurice Ewing Series 6, American Geophysical Union, Washington, D.C., 311–318.
- Anderson, J. G. (1991). A preliminary descriptive model for the distance dependence of the spectral decay parameter in southern California, *Bull. Seismol. Soc. Am.* **81**, 2186–2193.
- Anderson, J. G., and S. E. Hough (1984). A model for the shape of the Fourier amplitude spectrum of acceleration at high frequencies, *Bull. Seismol. Soc. Am.* **74**, 1969–1993.
- Anderson, J. G., and J. R. Humphrey Jr. (1991). A least squares method for objective determination of earthquake source parameters, *Seism. Res. Lett.* **62**, 201–209.
- Anderson, J. G., Y. Lee, Y. Zeng, and S. Day (1996). Control of strong motion by the upper 30 meters, *Bull. Seismol. Soc. Am.* **86**, 1749–1759.
- Andrews, M. C., W. D. Mooney, and R. P. Meyer (1985). The relocation of microearthquakes in the northern Mississippi Embayment, *J. Geophys. Res.* **90**, 10223–10236.
- Aoi, S., K. Obara, S. Hori, K. Kasahara, and Y. Okada (2000). New Japanese uphole–downhole strong-motion observation network: KiK-Net, *Seism. Res. Lett.* **72**, 239.
- Assimaki, D., W. Li, J. H. Steidl, and K. Tsuda (2008). Site amplification and attenuation via downhole array seismogram inversion: A comparative study of the 2003 Miyagi-oki aftershock sequence, *Bull. Seismol. Soc. Am.* **98**, 301–330.
- Aster, R. C., and P. M. Shearer (1991). High-frequency borehole seismograms recorded in the San Jacinto fault zone, southern California, Part 2: Attenuation and site effects, *Bull. Seismol. Soc. Am.* **81**, 1081–1100.
- Atkinson, G. M. (1996). The high-frequency shape of the source spectrum for earthquakes in eastern and western Canada, *Bull. Seismol. Soc. Am.* **86**, 106–112.
- Atkinson, G. M. (2004). Empirical attenuation of ground-motion spectral amplitudes in southeastern Canada and the northeastern United States, *Bull. Seismol. Soc. Am.* **94**, 1079–1095.
- Atkinson, G. M., and D. M. Boore (1995). New ground motion relations for eastern North America, *Bull. Seismol. Soc. Am.* **85**, 17–30.
- Atkinson, G. M., and D. M. Boore (1997). Some comparisons between recent ground-motion relations, *Seism. Res. Lett.* **68**, 24–40.
- Atkinson, G. M., and D. M. Boore (2006). Earthquake ground-motion prediction equations for eastern North America, *Bull. Seismol. Soc. Am.* **96**, 2181–2205.
- Barker, T. G., and J. L. Stevens (1983). Shallow shear wave velocity and Q structures at the El Centro strong-motion accelerograph array, *Geophys. Res. Lett.* **10**, 853–856.
- Barton, N. (2007). *Rock Quality, Seismic Velocity, Attenuation and Anisotropy*, Taylor & Francis, London.
- Beresnev, I. A., and G. M. Atkinson (1997). Shear-wave velocity survey of seismographic sites in eastern Canada: Calibration of empirical regression method of estimating site response, *Seism. Res. Lett.* **68**, 981–987.
- Beresnev, I. A., and G. M. Atkinson (1999). Generic finite-fault model for ground-motion prediction in eastern North America, *Bull. Seismol. Soc. Am.* **89**, 608–625.
- Bernreuter, D. L., J. B. Savy, R. W. Mensing, and J. C. Chen (1985). Seismic hazard characterization of 69 nuclear plant sites east of the Rocky Mountains, Rept. No. NUREG/CR-5250, Vol. 7, U.S. Nuclear Regulatory Commission, Washington, D.C.
- Boore, D. M. (1983). Stochastic simulation of high-frequency ground motions based on seismological models of the radiated spectra, *Bull. Seismol. Soc. Am.* **73**, 1865–1894.
- Boore, D. M. (1996). SMSIM—Fortran programs for simulating ground motions from earthquakes: Version 1.0, *U.S. Geol. Surv. Open-File Rept.* 96-80-A.
- Boore, D. M. (2003). Prediction of ground motion using the stochastic method, *Pure Appl. Geophys.* **160**, 635–676.
- Boore, D. M., and W. B. Joyner (1991). Estimation of ground motion at deep-soil sites in eastern North America, *Bull. Seismol. Soc. Am.* **81**, 2167–2185.
- Boore, D. M., and W. B. Joyner (1997). Site amplification for generic rock sites, *Bull. Seismol. Soc. Am.* **87**, 327–341.
- Boore, D. M., J. F. Gibbs, W. B. Joyner, J. C. Tinsley, and D. J. Ponti (2003). Estimated ground motion from the 1994 Northridge California, earthquake, at the site of the Interstate 10 and Las Cienega Boulevard bridge collapse, West Los Angeles, California, *Bull. Seismol. Soc. Am.* **93**, 2737–2751.
- Bonilla, L. F., J. H. Steidl, J. C. Gariel, and R. J. Archuleta (2002). Borehole response studies at the Garner Valley downhole array, southern California, *Bull. Seismol. Soc. Am.* **92**, 3165–3179.

- Borcherdt, R. D. (1994). Estimates of site-dependent response spectra for design (methodology and justification), *Earthq. Spectra* **10**, 617–653.
- Brune, J. (1970). Tectonic stress and the spectra of seismic shear waves, *J. Geophys. Res.* **75**, 4997–5009.
- Brune, J. (1971). Correction: Tectonic stress and the spectra of seismic shear waves, *J. Geophys. Res.* **76**, 5002.
- Building Seismic Safety Council (BSSC) (2004). NEHRP recommended provisions for seismic regulations for new buildings and other structures (FEMA 450), 2003 Ed., *National Institute of Building Sciences*, Washington, D.C.
- Campbell, K. W. (2003). Prediction of strong ground motion using the hybrid empirical method and its use in the development of ground-motion (attenuation) relations in eastern North America, *Bull. Seismol. Soc. Am.* **93**, 1012–1033.
- Campbell, K. W. (2004). Erratum: Prediction of strong ground motion using the hybrid empirical method and its use in the development of ground-motion (attenuation) relations in eastern North America, *Bull. Seismol. Soc. Am.* **94**, 2418.
- Campbell, K. W. (2007). Validation and update of hybrid empirical ground motion (attenuation) relations for the CEUS, NEHRP external research program, Final Technical Rept., *U.S. Geol. Surv. Award No. 05HQGR0032*.
- Chang, T. S., L. K. Teh, and Y. Zhang (1992). Seismic characteristics of sediments in the New Madrid seismic zone, Open-File Rept., *Center for Earthquake Research and Information*, Memphis State University, Memphis, Tennessee.
- Chapman, M. C., J. R. Martin, C. G. Olgun, and J. N. Beale (2006). Site-response models for Charleston, South Carolina, and vicinity developed from shallow geotechnical investigations, *Bull. Seismol. Soc. Am.* **96**, 467–489.
- Chapman, M. C., P. Talwani, and R. C. Cannon (2003). Ground-motion attenuation in the Atlantic Coastal Plain near Charleston, South Carolina, *Bull. Seismol. Soc. Am.* **93**, 998–1011.
- Chen, K. C., J. M. Chiu, and Y. T. Yang (1994). $Q_p - Q_s$ relation in the sedimentary basin of the upper Mississippi Embayment using converted phases, *Bull. Seismol. Soc. Am.* **84**, 1861–1868.
- Chen, K. C., J. M. Chiu, and Y. T. Yang (1996). Shear-wave velocity of the sedimentary basin in the upper Mississippi Embayment using S-to-P converted waves, *Bull. Seismol. Soc. Am.* **86**, 848–856.
- Clouser, R. H., and C. A. Langston (1991). $Q_p - Q_s$ relations in a sedimentary basin using converted phases, *Bull. Seismol. Soc. Am.* **81**, 733–750.
- Cormier, V. F. (1982). The effect of attenuation on seismic body waves, *Bull. Seismol. Soc. Am.* **72**, S169–S200.
- Cramer, C. H., J. S. Gombert, E. S. Schweig, B. A. Waldron, and K. Tucker (2004). The Memphis, Shelby County, Tennessee, seismic hazard maps, *U.S. Geol. Surv. Open-File Rept. 04-1294*.
- Dainty, A. M. (1981). A scattering model to explain seismic Q observations in the lithosphere between 1 and 30 Hz, *Geophys. Res. Lett.* **8**, 1126–1128.
- Daley, T. M., and T. V. McEvelly (1990). Shear-wave anisotropy in the Parkfield Varian well VSP, *Bull. Seismol. Soc. Am.* **80**, 857–869.
- Dobry, R., R. D. Borcherdt, C. B. Crouse, I. M. Idriss, W. B. Joyner, G. R. Martin, M. S. Power, E. E. Rinne, and R. B. Seed (2000). New site coefficients and site classification system used in recent building seismic code provisions, *Earthq. Spectra* **16**, 41–67.
- Drnevich, V. P., and F. E. Richart Jr. (1970). Dynamic prestraining of dry sand, *J. Soil Mech. Found. Div. ASCE* **96**, 453–469.
- Electrical Power Research Institute (EPRI) (1993). Methods and guidelines for estimating earthquake ground motion in eastern North America, in *Guidelines for Determining Design Basis Ground Motions*, EPRI Rept. No. TR-102293, Vol. 1, Palo Alto, California.
- Electrical Power Research Institute (EPRI) (2004). CEUS ground motion project final report, EPRI Rept. No. TR-1009684, Palo Alto, California.
- Fehler, M., P. Roberts, and T. Fairbanks (1988). A temporal change in coda wave attenuation observed during an eruption of Mount St. Helens, *J. Geophys. Res.* **93**, 4367–4373.
- Fletcher, J. B. (1995). Source parameters and crustal Q for four earthquakes in South Carolina, *Seism. Res. Lett.* **66**, no. 4, 44–58.
- Fletcher, J. B., T. Fumal, H. P. Liu, and L. C. Carroll (1990). Near-surface velocities and attenuation at two boreholes near Anza, California, from logging data, *Bull. Seismol. Soc. Am.* **80**, 807–831.
- Frankel, A., and R. W. Clayton (1986). Finite difference simulations of seismic scattering: Implications for the propagation of short-period seismic waves in the crust and models of crustal heterogeneity, *J. Geophys. Res.* **91**, 6465–6489.
- Frankel, A., and L. Wennerberg (1987). Energy-flux model of seismic coda: Separation of scattering and intrinsic attenuation, *Bull. Seismol. Soc. Am.* **77**, 1223–1251.
- Frankel, A., C. Mueller, T. Barnhard, D. Perkins, E. Leyendecker, N. Dickman, S. Hanson, and M. Hopper (1996). National seismic hazard maps: Documentation June 1996, *U.S. Geol. Surv. Open-File Rept. 96-532*.
- Frankel, A. D., M. D. Petersen, C. S. Mueller, K. M. Haller, R. L. Wheeler, E. V. Leyendecker, R. L. Wesson, S. C. Harmsen, C. H. Cramer, D. M. Perkins, and K. S. Rukstales (2002). Documentation for the 2002 update of the national seismic hazard maps, *U.S. Geol. Surv. Open-File Rept. 02-420*.
- Futterman, W. I. (1962). Dispersive body waves, *J. Geophys. Res.* **67**, 5279–5291.
- Gardner, G. H. F., M. R. J. Wyllie, and D. M. Droschak (1964). Effects of pressure and fluid saturation on the attenuation of elastic waves in sands, *J. Pet. Techn.* **16**, 189–198.
- Ge, J., J. Pujol, S. Pezeshk, and S. Stovall (2009). Determination of shallow shear wave attenuation in the Mississippi Embayment using vertical seismic profiling data, *Bull. Seismol. Soc. Am.* **99**, no. 3, 1636–1649.
- Gibbs, J., and E. Roth (1989). Seismic velocities and attenuation from borehole measurements near the Parkfield prediction zone, central California, *Earthq. Spectra* **5**, 513–537.
- Gibbs, J., D. Boore, W. Joyner, and T. Fumal (1994). The attenuation of seismic shear waves in Quaternary alluvium in Santa Clara Valley, California, *Bull. Seismol. Soc. Am.* **84**, 76–90.
- Gombert, J., B. Waldron, E. Schweig, H. Hwang, A. Webbbers, R. Van Arsdale, K. Tucker, R. Williams, R. Street, P. Mayne, W. Stephenson, J. Odum, C. Cramer, R. Updike, S. Hutson, and M. Bradley (2003). Lithology and shear-wave velocity in Memphis, Tennessee, *Bull. Seismol. Soc. Am.* **93**, 986–997.
- Hallidorsson, B., and A. S. Papageorgiou (2005). Calibration of the specific barrier model to earthquakes of different tectonic regions, *Bull. Seismol. Soc. Am.* **95**, 1276–1300.
- Hanks, T. C. (1982). f_{max} , *Bull. Seismol. Soc. Am.* **72**, 1867–1879.
- Hanks, T. C., and R. K. McGuire (1981). The character of high frequency strong ground motion, *Bull. Seismol. Soc. Am.* **71**, 2071–2095.
- Harris, J. B., and R. L. Street (1997). Seismic investigation of near-surface geological structure in the Paducah, Kentucky, area: Application to earthquake hazard evaluation, *Eng. Geol.* **46**, 369–383.
- Hartzell, S., S. Harmsen, A. Frankel, D. Carver, E. Cranswick, M. Meremonte, and J. Michael (1998). First-generation site-response maps for the Los Angeles region based on earthquake ground motions, *Bull. Seismol. Soc. Am.* **88**, 463–472.
- Hartzell, S., A. Leeds, A. Frankel, and J. Michael (1996). Site response for urban Los Angeles using aftershocks of the Northridge earthquake, *Bull. Seismol. Soc. Am.* **86**, S168–S192.
- Haskell, N. A. (1960). Crustal reflection of plane SH waves, *J. Geophys. Res.* **65**, 4147–4150.
- Hauksson, E., T. L. Teng, and T. L. Henyey (1987). Results from a 1500 m deep, three-level downhole seismometer array: Site response, low Q values, and f_{max} , *Bull. Seismol. Soc. Am.* **77**, 1883–1904.
- Hough, S. E., and J. G. Anderson (1988). High-frequency spectra observed at Anza, California: Implications of Q structure, *Bull. Seismol. Soc. Am.* **78**, 692–707.
- Hough, S. E., J. G. Anderson, J. Brune, F. Vernon III, J. Berger, J. Fletcher, L. Haar, T. Hanks, and L. Baker (1988). Attenuation near Anza, California, *Bull. Seismol. Soc. Am.* **78**, 672–691.

- Hwang, H. H. M., H. Lin, and J.-R. Huo (1997). Site coefficients for design of buildings in eastern United States, *Soil Dyn. Earthq. Eng.* **16**, 29–40.
- International Code Committee (ICC) (2006). International building code: Code and commentary, 2006 Edition, Vols. **1,2**, Falls Church, Virginia.
- Johnston, D. H., and M. N. Toksoz (1980a). Ultrasonic P and S wave attenuation in dry and saturated rocks under pressure, *J. Geophys. Res.* **85**, 925–936.
- Johnston, D. H., and M. N. Toksoz (1980b). Thermal cracking and amplitude dependent attenuation, *J. Geophys. Res.* **85**, 937–942.
- Johnston, D. H., M. N. Toksoz, and A. Timur (1979). Attenuation of seismic waves in dry and saturated rocks, Part II: Mechanisms, *Geophysics* **44**, 691–711.
- Jongmans, D., and P. E. Malin (1995). Vertical profiling of microearthquake S waves in the Varian well at Parkfield, California, *Bull. Seismol. Soc. Am.* **85**, 1805–1820.
- Joyner, W. B., R. E. Warrick, and T. E. Fumal (1981). The effect of Quaternary alluvium on strong ground motion in the Coyote Lake, California, earthquake of 1979, *Bull. Seismol. Soc. Am.* **71**, 1333–1349.
- Kanai, K. (1983). *Engineering Seismology*, University of Tokyo Press, Tokyo.
- Kanamori, H. (1967). Spectrum of short-period core phases in relation to the attenuation in the mantle, *J. Geophys. Res.* **72**, 2181–2186.
- Kang, I. B., and G. A. McMechan (1994). Separation of intrinsic and scattering Q based on frequency-dependent amplitude ratios of transmitted waves, *J. Geophys. Res.* **99**, 23875–23885.
- Kinoshita, S. (2008). Deep-borehole-measured Q_P and Q_S attenuation for two Kanto sediment layer sites, *Bull. Seismol. Soc. Am.* **98**, 463–468.
- Knopoff, L. (1964). Q , *Rev. Geophys. Space Phys.* **2**, 625–660.
- Kramer, S. L. (1996). *Geotechnical Earthquake Engineering*, Prentice Hall, Upper Saddle River, New Jersey.
- Kudo, K., and E. Shima (1970). Attenuation of shear waves in soil, *Bull. Earthq. Res. Inst.* **48**, 145–148.
- Lai, C. G., G. J. Rix, S. Foti, and V. Roma (2002). Simultaneous measurement and inversion of surface wave dispersion and attenuation curves, *Soil Dyn. Earthq. Eng.* **22**, 923–930.
- Langston, C. A. (2003a). Local earthquake wave propagation through Mississippi Embayment sediments, Part I: Body wave phases and local site responses, *Bull. Seismol. Soc. Am.* **93**, 2664–2684.
- Langston, C. A. (2003b). Local earthquake wave propagation through Mississippi Embayment sediments, Part II: Influence of local site velocity structure on Q_P and Q_S determinations, *Bull. Seismol. Soc. Am.* **93**, 2685–2702.
- Langston, C. A., P. Boden, C. Powel, M. Withers, S. Horton, and W. Mooney (2005). Bulk sediment Q_P and Q_S in the Mississippi Embayment, central United States, *Bull. Seismol. Soc. Am.* **95**, 2162–2179.
- Lay, T., and T. C. Wallace (1995). *Modern Global Seismology*, Academic Press, San Diego, California.
- Lee, R. C., M. D. Hood, and M. R. Lewis (2007). Savannah River Site probabilistic seismic hazard assessment update (U), *Rept. No. WSRC-TR-2006-00113*, Westinghouse Savannah River Company, Aiken, Georgia.
- Lee, R. C., M. E. Maryak, and M. D. McHood (1997). SRS seismic response analysis and design basis guidelines, *Rept. No. WSRC-TR-97-0085*, Westinghouse Savannah River Company, Aiken, Georgia.
- Liu, Z., M. E. Wuenschel, and R. B. Herrmann (1994). Attenuation of body waves in the central New Madrid seismic zone, *Bull. Seismol. Soc. Am.* **84**, 1112–1122.
- Magistrale, H., K. McLaughlin, and S. Day (1996). A geology-based 3D velocity model of the Los Angeles basin sediments, *Bull. Seismol. Soc. Am.* **86**, 1161–1166.
- Moos, D., and M. D. Zoback (1983). In situ studies of seismic velocity in fractured crystalline rocks, *J. Geophys. Res.* **88**, 2345–2358.
- Mori, J., and A. Frankel (1991). Depth dependent scattering shown by coherence estimates and regional coda amplitudes, *EOS (Suppl.)* **72**, 344.
- Morozov, I. B. (2008). Geometrical attenuation, frequency dependence of Q , and the absorption band problem, *Geophys. J. Int.* **175**, 239–252.
- Morozov, I. B. (2009). Thirty years of confusion around “scattering Q ”? *Seism. Res. Lett.* **80**, 5–7.
- Papageorgiou, A. S., and K. Aki (1983). A specific barrier model for the quantitative description of inhomogeneous faulting and the prediction of strong ground motion, Part II: Applications of the model, *Bull. Seismol. Soc. Am.* **73**, 953–978.
- Park, D., and Y. M. A. Hashash (2004). Evaluation of seismic site factors in the Mississippi Embayment, Part I: Estimation of dynamic properties, *Soil Dyn. Earthq. Eng.* **25**, 133–144.
- Petersen, M. D., A. D. Frankel, S. C. Harmsen, C. S. Mueller, K. M. Haller, R. L. Wheeler, R. L. Wesson, Y. Zeng, O. S. Boyd, D. M. Perkins, N. Luco, E. H. Field, C. J. Wills, and K. S. Rukstales (2008). Documentation for the 2008 update of the United States national seismic hazard maps, *U.S. Geol. Surv. Open-File Rept. 2008-1128*.
- Pujol, J., S. Pezeshk, Y. Zhang, and C. Zhao (2002). Unexpected values of Q_S in the unconsolidated sediments of the Mississippi Embayment, *Bull. Seismol. Soc. Am.* **92**, 1117–1128.
- Pullii, J. J. (1984). Attenuation of coda waves in New England, *Bull. Seismol. Soc. Am.* **74**, 1149–1166.
- Redpath, B. B., and R. C. Lee (1986). In-situ measurements of shear-wave attenuation at a strong-motion recording site, NEHRP external research program, *U.S. Geol. Survey Final Technical Rept., Contract No. 14-08-001-21823*.
- Redpath, B. B., R. B. Edwards, R. J. Hale, and F. C. Kintzer (1982). Development of field techniques to measure damping values for shallow rocks and soils, *Rept. No. URS/JAB 7941*, URS/Blume Engineers, San Francisco, California.
- Rix, G. J., C. G. Lai, and A. W. Spang Jr. (2000). In situ measurement of damping ratio using surface waves, *J. Geotech. Geoenviron. Eng.* ASCE **126**, 472–480.
- Romero, S. M., and G. J. Rix (2001). Ground motion amplification in the upper Mississippi Embayment, *Rept. No. GIT-CEE/GEO-01-1*, School of Civil and Environmental Engineering, Georgia Institute of Technology, Atlanta, Georgia.
- Sato, H., M. Fehler, and R. S. Wu (2002). Scattering and attenuation of seismic waves in the lithosphere, in *International Handbook of Earthquake & Engineering Seismology*, W. H. K. Lee, H. Kanamori, P. C. Jennings, and C. Kisslinger (Editors), Part A, Academic Press, San Diego, California.
- Savy, J. B., D. L. Bernreuter, and J. C. Chen (1987). A methodology to correct for effect of the local site characteristics in seismic hazard analyses, in *Ground Motion and Engineering Seismology*, A. S. Cakmak (Editor), Developments in Geotechnical Engineering, Vol. **44**, Elsevier, Amsterdam, 243–255.
- Silva, W. J., and R. Darragh (1995). Engineering characterization of earthquake strong ground motion recorded at rock sites, *EPRI Rept. No. TR-102261*, Electric Power Research Institute, Palo Alto, California.
- Silva, W., N. Gregor, and R. Darragh (2003). Development of regional hard rock attenuation relations for central and eastern North America, mid-continent, and Gulf Coast areas, Pacific Engineering and Analysis, El Cerrito, California.
- Silva, W. J., S. Li, R. Darragh, and N. Gregor (1999a). Surface geology based strong motion amplification factors for the San Francisco Bay and Los Angeles areas, *Final Rept., Pacific Earthquake Engineering Research Center*, University of California, Berkeley, California.
- Silva, W., R. Darragh, N. Gregor, G. Martin, N. Abrahamson, and C. Kircher (1999b). Reassessment of site coefficients and near-fault factors for building code provisions, NEHRP external research program, *U.S. Geol. Survey Final Technical Rept., Award No. 98HQGR1010*.
- Somerville, P., N. Collins, N. Abrahamson, R. Graves, and C. Saikia (2001). Ground motion attenuation relations for the central and eastern United States, NEHRP external research program, *U.S. Geol. Survey Final Technical Rept., Award No. 99HQGR0098*.
- Tavakoli, B., and S. Pezeshk (2005). Empirical-stochastic ground-motion prediction for eastern North America, *Bull. Seismol. Soc. Am.* **95**, 2283–2296.

- Toro, G. R. (2002). Modification of the Toro et al. (1997) attenuation equations for large magnitudes and short distances, Risk Engineering, Boulder, Colorado.
- Toro, G. R., N. A. Abrahamson, and J. F. Schneider (1997). Model of strong ground motions from earthquakes in central and eastern North America: Best estimates and uncertainties, *Seism. Res. Lett.* **68**, 41–57.
- Vernon, F. L., G. L. Pavlis, T. J. Owens, D. E. McNamara, and P. N. Anderson (1998). Near-surface scattering effects observed with a high-frequency phased array at Pinyon Flats, California, *Bull. Seismol. Soc. Am.* **88**, 1548–1560.
- Wald, L., and J. Mori (2000). Evaluation of methods for estimating linear site-response magnification in the Los Angeles region, *Bull. Seismol. Soc. Am.* **90**, S32–S42.
- Wang, Z., R. Street, E. Woolery, and J. Harris (1994). Q_S estimation for unconsolidated sediments using first-arrival *SH* wave critical refractions, *J. Geophys. Res.* **99**, 13543–13551.
- Wen, Y. K., and C. L. Wu (2001). Uniform hazard ground motions for mid-America cities, *Earthq. Spectra*, **17**, 359–384.
- Wennerberg, L., and A. Frankel (1989). On the similarity of theories of anelastic and scattering attenuation, *Bull. Seismol. Soc. Am.* **79**, 1287–1293.
- Whitman, R. V., and F. E. Richart Jr. (1967). Design procedures for dynamically loaded foundations, *J. Soil Mech. Found. Div. ASCE* **93**, 169–193.
- Wuenschel, M. E., R. B. Herrmann, and Z. Liu (1991). Attenuation of body waves in the New Madrid seismic zone, *Seism. Res. Lett.* **62**, 191.

EQECAT, Inc.
1030 NW 161st Place
Beaverton, Oregon 97006
KCcampbell@eqecat.com

Manuscript received 1 November 2007